

This document includes authors' responses to both reviewer 1 and reviewer 2. Reviewer's comments are in bold text. Authors' responses are plain text with any text taken from the manuscript in italics. New additions to the manuscript in response to reviewer comments are shown in red italics.

Response to RC1: Anonymous Referee #1

General comment: The work by Squires et al. presents traffic related pollutant emissions in an Asian megacity. It presents novel data for a globally important region struggling with air quality. The manuscript is appropriate for publication in ACP after addressing some of the more specific comments outlined below.

The authors thank the reviewer for the supportive comments and taking the time to review the manuscript.

Specific comments: Section 2.4: It is not entirely clear how the data treatment is done. Were the data time-shifted before submitting these to the eddy flux routine or did the eddy flux routine take account this shift and perform a covariance analysis? A better approach to deal with lag-time estimation when individual 30 min covariance functions are below the LOD (to estimate a lag time) is to average quality filtered covariance functions. This allows to obtain a study (or weekly) average lag time for each individual species. This is a more accurate approach if compounds exhibit different absorption and desorption properties along an inlet line.

We calculated the lag times for NO_x and CO data for each 30 minute period, by cross-covariance maximisation between pollutant concentration and vertical wind speed. When determining the lag time for each species a high-pass filter (Hartmann et al., 2018) is used which improves the precision of the determined lag time by an order of magnitude. As recommended, we then further calculated the median lag times for each species based only on high quality fluxes for each campaign. We performed the lag-time shift using these median values for each campaign.

We added more details to section 2.4 of the manuscript to make the data treatment clearer and have included the standard deviation when reporting median lag times.

*Concentration data were coupled with wind data reported by the sonic anemometer by sub-sampling the wind vector data to match the 5 Hz concentration data. Data were then despiked prior to flux calculation as per the method described in Brock (1986) and Starkenburg et al. (2016). Following despiking, the lag time between vertical wind velocity measured in-situ on the tower and the pollutant concentrations, measured on the ground, was calculated. **The lag time correction was determined by maximisation of the cross-covariance between pollutant concentration and the vertical wind component. When determining the lag time for each species a high-pass filter (Hartmann et al., 2018) was used which improves the precision of the determined lag time by an order of magnitude. The median lag time was then calculated for each species during each campaign. The lag time between the concentration and vertical wind speed during the winter campaign was found to be 9.6 ± 0.4 s, 10.0 ± 0.4 s, 10.2 ± 0.3 s for NO, NO₂ and CO respectively. For the summer campaign lag times were calculated as 9.4 ± 0.4 s, 9.8 ± 0.3 s and 10.6 ± 0.5 s. Because there was no discernible pattern or trend in the lag-times and to prevent the flux bias that cross-covariance maximisation can introduce when fluxes are small (Langford et al., 2015), the final fluxes were calculated by applying the median time-lag value for each campaign to all flux periods.***

Section 2.5: Line 6, 16: The authors should outline the changes incorporated in eddy4R that were specifically implemented and necessary for the present study (e.g. by showing a work flow diagram). Flux footprint model. The flux footprint model is based on Kljun et al., 2004 and was modified

according to Metzger et al. 2012. Kljun et al. 2012 updated their original footprint model. It is not clear what the exact differences between the cross-integrated footprints between Kljun et al. 2012 and Metzger et al. 2012 are, assuming they are not the same. A clarification of this issue would be warranted.

A workflow diagram (shown below) has been added to the manuscript which highlights the key stages in the flux processing workflow, with any settings specific to the Beijing campaign processing noted.

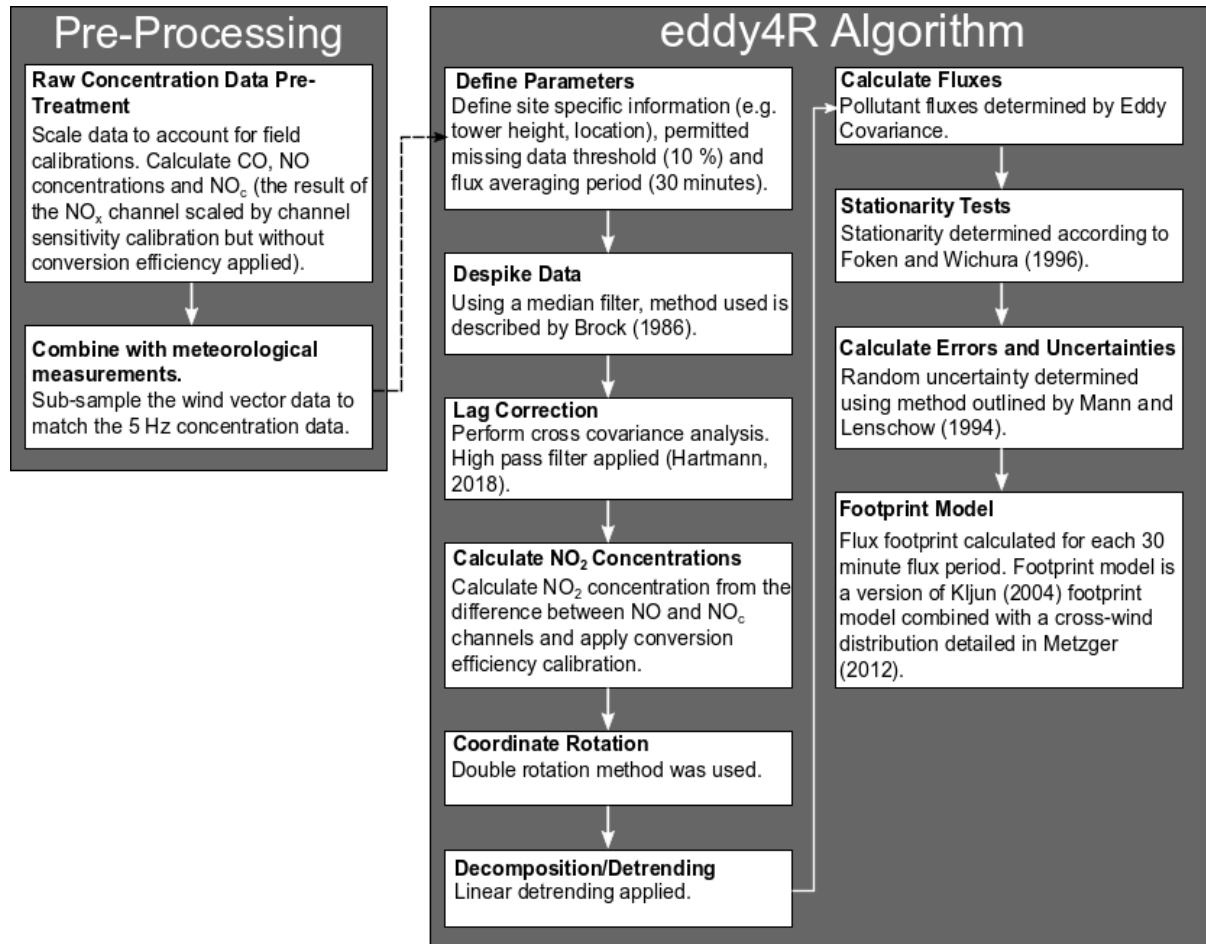


Figure 2. Workflow schematic summarising the data processing steps required for calculation of NO_x and CO fluxes.

The flux footprint model is based on Kljun et al. (2004) with the modifications described in Metzger et al. (2012; K04). A short description of the model is included in the workflow diagram and this description has been added to section 2.6 to clarify the model set up used.

The footprint model used is described in detail in Kljun et al. (2004) and Metzger et al. (2012). The footprint model used is based on Kljun et al. (2004) with a cross-wind distribution detailed in Metzger et al. (2012).

We used this model as it performed reliably during various flux footprint model inter-comparisons, including in comparisons with the model described in Kljun et al. (2015; K15), which updated the model described in Kljun et al. (2004). Heidbach et al. (2017) use a tracer experiment to evaluate flux footprint models, including Kormann and Meixner (2001; KM01) and K15. Metzger et al. (2012) on the other hand use a Lagrangian particle model to evaluate KM01 and Kljun et al. (2004) including the cross-wind distribution that is used in this work (K04). In addition, Heidbach et al. (2011) evaluated KM01 and K04 over extensive field data. Using KM01 as a common benchmark among these studies,

one can see similar improvements of K15 and K04 over KM01, including in the cross-wind integrated footprints.

Section 2.7: Page 9: “For this evaluation, an optimized version of the MEIC v1.3 inventory for 2013 was used that was derived by fitting the NAQPMS model with observed pollutant concentrations during the campaign periods.” What was done explicitly to optimize the MEIC inventory here. The authors cite a reference, but it would help the reader to understand the approach if more information on the procedure was given here.

This was an oversight; the optimized emissions referred to here and in the paper cited were not used in the final version of the analysis, which is based on the standard MEIC v1.3 emissions from 2013. This sentence has now been removed from the paper. The section now reads:

The measured pollutant fluxes were compared with the Multi-resolution Emissions Inventory for China (MEIC, Qi et al. (2017), <http://www.meicmodel.org/>, last access: 19 May 2020) to evaluate how well the inventory describes the diurnal evolution of pollutants and their absolute magnitude. MEIC emissions are available at 0.25×0.25 degree resolution and were downscaled to 3×3 km resolution on a sector by sector basis following the approach of Zheng et al. (2017). MEIC considers five emission source sectors; power plants, industry, transport, residential, and agricultural. Agricultural emissions are not relevant within our flux footprint so were not included in this work. Emissions are available on a monthly basis, and are assumed to be the same each day of the month, and a diurnal cycle appropriate to Chinese sources is applied to each emission sector. Example emissions for Beijing are presented in figure A3 for November.

More details have been added to the same section to describe how MEIC emissions were compared with the measured emissions:

The NO_x and CO emission predicted by the inventory are calculated from the multiplication of each footprint matrix by the MEIC grid. In order to match the scales of the footprint matrix and the inventory, a pseudo $100 \text{ m} \times 100 \text{ m}$ MEIC grid was created by splitting the 3 km resolution inventory into smaller $100 \text{ m} \times 100 \text{ m}$ grid squares, each with the same emission value.

Section 3.1: In this manuscript fluxes are generally reported as $\text{mg}/\text{m}^2/\text{h}$. How was the NO_x flux derived in units of $\text{mg}/\text{m}^2/\text{h}$? The NO_x channel would strictly only allow to report fluxes on a molar basis. Partitioning NO_x and NO fluxes from the two channels could introduce additional uncertainty.

NO_x flux was reported in mass units from the sum of the NO and NO_2 mass fluxes. Because the measurement of NO_2 is determined by two distinct channels, any difference in response time between the channels would mean a NO_2 concentration could not be accurately determined. To account for this and derive NO_2 fluxes accurately, NO_2 concentrations were calculated after the lag time shift had been applied. Because the path lengths of the instruments are identical the lag difference between the channels was very small but could have had an impact when data is recorded at 5 Hz.

More details have been added to the “Data Processing” section (shown below) and these steps are included in the new workflow diagram to make this clear.

Prior to the calculation of pollutant fluxes, the raw data were scaled to take account of calibrations. The sensitivity within each channel of the NO_x chemiluminescence instrument remained consistent throughout the winter and summer campaigns so data were scaled using median sensitivity values. The conversion efficiency of the NO_x channel gradually deteriorated over the two campaigns and so NO_2 data were scaled using linearly interpolated conversion efficiency values. As highlighted in Fig. 2, the NO_2 calibration was applied in two stages, the first during pre-processing and the second following

lag correction. During the pre-processing stage the channel sensitivities (counts pptv⁻¹) determined by field calibration are applied to both the NO and NO_x channels to give NO (pptv) and a term referred to as converted NO_x channel counts 'NO_c'. NO₂ is then calculated from the difference between the time-lagged corrected NO_c and NO divided by conversion efficiency. The time lag correction is described below.

Tower setup: at the height of the tower one would expect that the measurements are decoupled from the surface and represent the residual layer during night. How is this taken into account into the interpretation of night time data? Could this influence the storage flux calculation for night time?

Measurements of the boundary layer height (BLH) were used to filter out any data where the BLH dropped to 30 m above measurement height or below, described in the manuscript:

...any periods where the boundary layer was within 30 m above the measurement height were removed from the data.

Only measurements made within the BL are therefore included in the calculations. BLH measurements showed that the measurement height was decoupled on some but by no means all nights, helped by the nocturnal heat output from the city. In addition, we assessed the validity of the single-height storage flux calculation. In addition to the NO_x, CO and aromatic VOC fluxes described in this work there were parallel flux measurements of other species, including CO₂ flux, which will be described in upcoming publications. For CO₂ we had access to simultaneous concentration profile measurements on the tower at three heights for a period during the summer campaign and compared a storage flux calculation based on a multi-height profile with that based on our single-height observations at the flux measurement height (Eq. (2)). We found excellent agreement and no systematic bias. As with any urban flux measurement (and independent of measurement height), we cannot completely rule out that storage might interact with low-level advection during nighttime and, for the reactive tracers, also with chemistry. More details have been added to the manuscript to clarify the method used to evaluate the storage flux calculation:

The validity of calculating the storage flux at a single measurement height was evaluated by comparing CO₂ concentration measurements made at the measurement height and CO₂ concentration profile measurements made at three different heights on the tower. By comparing the evolution of the CO₂ concentration at the single measurement height with the CO₂ profile measurements, it was determined that calculating storage flux using the single concentration at the measurement height was a reasonable approximation of the storage within the column.

Table 1: Additional measurements where BTEX fluxes were reported directly should be included in Table 1. For example, Karl et al. 2018 (10.1073/pnas.1714715115) report 24h average benzene (toluene) fluxes of 20 (82) ug/m²/h for Innsbruck. Park et al., 2010 (10.1016/j.atmosenv.2010.04.016) present BTEX fluxes for Houston with maximum daytime fluxes in the range of 0.2-0.3 mg/m²/h and 0.5 -0.7 mg/m²/h.

These references have been added to Table 1.

Editorial comments: Page 1: line 1: fluxes? Page 2: line 12 cc PM can also be emitted by primary sources, depending on size, primary or secondary production is more relevant. As Chinese efforts to reduce primary PM are regarded successful, a reference could be given to what extent secondary aerosols are nowadays dominating in a city like Beijing Page 2: line 15 is a repetition of what was said a couple of lines earlier – it could be rewritten more concisely Page 2: line 18: “At” high

concentration Page 5: line 17: : : : was also. : : : ! Page 6: line 7 cc: this is not a complete sentence. Page 7: line 17: Fig. A1, Fig. A2: : : . Page 8: line 10: : : :.tower tower: : : . Page 8: line 30:: : : . to THE measured flux ? General editorial comments. Naming and formatting of figures, tables and references should follow the ACP editorial guidelines and should be copy edited. For example many references are cited as" by (Famulari et al, 2010;): : : ." Probably due to the citation software used. ACP formatting guidelines however suggest to cite as following: by Famulari et al. (2010). Similarly, references to figures do not follow ACP formatting guidelines and should be corrected.

These editorial changes have been made and a reference added to the introduction to highlight the importance of secondary aerosol in Beijing.

Secondary aerosols have been shown to comprise a large fraction of fine particulate matter in Beijing (Guo et al., 2014; Duan et al., 2020).

Response to RC2: Anonymous Referee #2

Squires et al. describe seasonal differences in flux measurements of CO, NO_x, and select VOCs in Beijing during winter and summer, 2016-2017. The authors show that seasonal differences in combustion markers can be largely attributed to changing sources between the two seasons (residential vs. transportation), while changes in the fluxes of aromatic VOCs are strongly influenced by evaporative emissions during summer. The authors compare the flux measurements to inventory estimates from the MEIC, and discuss the significant discrepancies between the measurements and the inventory. The authors also use the inventory to infer how seasonal differences in emission sectors may have contributed to the observed seasonality in CO and NO_x fluxes.

Overall, the manuscript is very well written and organized, and the authors tell a compelling story as to what contributes to the CO, NO_x, and VOC sources observed in Beijing. It is also an important contribution to constraining emission inventories in China, which evolve quickly as sources continue to face regulations. The manuscript should be published in ACP, provided that the authors address a few comments pertaining to the comparison of the measurements and inventory.

The authors thank reviewer 2 for their complimentary and supportive comments and for taking the time to review the manuscript.

Main Comments

1. **Section 3.4.** I appreciate the authors' careful discussion and source attribution of the VOC fluxes, since this can be more complicated than for CO and NO_x due to the variety of processes that could contribute to enhanced VOC fluxes (emissions, temperature, etc.). I am impressed by the general higher flux of aromatics in the summer and good correlation with heat flux. This seems to suggest that evaporative emissions are a driving factor in the behavior of the aromatics (as concluded by the authors), and could be the primary explanation in the seasonal differences in B/T ratios. The authors note that a detailed comparison of the VOC emissions with the inventory is beyond the scope of the work (which is reasonable), but is it possible to do a comparison between the aromatic / benzene ratios measured in this work with VOC profiles represented in the MEIC or other inventories? Li et al. (2017) tends to show that residential uses of aromatics result in higher emissions than the transportation sector. Perhaps a comparison of the B/T ratio between sectors would provide additional evidence as to what is contributing to these seasonal differences.

This is a very good suggestion. Unfortunately, in the MEIC inventory benzene and toluene are grouped together as one emission value as described in Acton et al. (2020). It is therefore not possible to calculate aromatic/benzene ratios using the MEIC inventory. Given the focus of this work the authors consider a comparison with a different inventory to be out of scope. The manuscript states observed B/T ratios with a view to highlighting seasonal differences in emission sources. A reference has been added to highlight the probable contribution of fuel evaporation in the summer leading to the lower B/T emission ratios observed:

Indeed, Karl et al. (2009) showed that fuel evaporative losses typically have a higher toluene fraction, leading to lower B/T ratios. The strong VOC-heat flux correlation and the low B/T ratio observed during the summer campaign suggests fuel evaporative loss is a source of aromatic VOC emissions in Beijing.

2. **Section 3.5 and Figure 9.** In this section, the authors discuss the measurements in context with the MEIC. The discussion of this section largely hinges on Figure 9, which suggests that

the inventory largely overestimates NO_x and CO emissions. In my opinion, this figure is misleading, since this is comparing an inventory from 2013 to measurements conducted in 2017. The authors note later in the section that the NO_x and CO emissions in China change drastically on a multi-year basis. The authors discuss how these changes would have likely affected the MEIC estimates from 2013, but still conclude that the inventory is overestimated.

I think that it would be most fair to structure this section to first show how the inventory would have changed from 2013 until 2017, then adjust the inventory estimates appropriately to account for these CO and NO_x reductions, and finally compare these profiles to the measurements conducted in 2017 and discuss the discrepancies. Otherwise, a reader who skims the figures might conclude that the inventory is entirely out to lunch, which isn't truly the case.

This section has been restructured to introduce the adjusted inventory before the discussion of uncertainties due to spatial proxies. Figure 9 (in original manuscript, now figure 10 due to the addition of a new figure) has been changed to show the adjusted inventory rather than the original.

The structure of section 3.5 is now as follows:

- Comparisons with the unadjusted inventory and measured NO_x and CO emissions are stated.
- There is a discussion of changes in emissions for Beijing between 2013 (base year of the inventory) and 2016/2017 (years measurements were made), concluding that NO_x and CO emissions should be reduced by 30 % for 2016 and 43 % for 2017.
- The inventory is adjusted accordingly and compared to measured emissions. The comparison is presented in a new version of figure 9 (now figure 10).
- The diurnal variation in emissions and seasonal differences within the inventory are discussed as in the original manuscript.

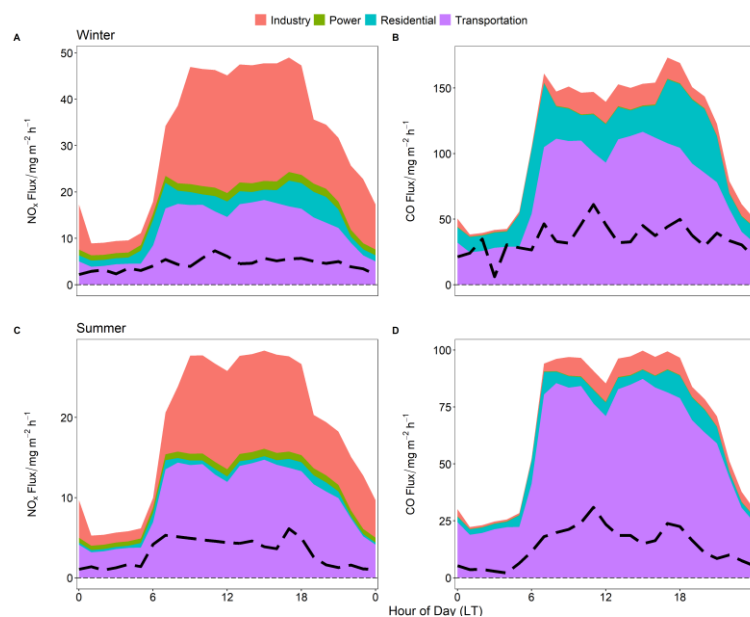


Figure 10: Measured diurnal trend (dashed black line) and predicted diurnal trend using the MEIC inventory (filled areas by sector) for NO_x and CO emissions. MEIC inventory data has been reduced by 30 % for comparison with the winter 2016 campaign and by 43 % for comparison with the summer 2017 campaigns to take account of expected emissions reductions indicated in Cheng et al. (2019). Panels A and B show emissions for the winter campaign and panels C and D show emissions from the summer campaign.

Other Comments

3. Page 2, Lines 25 - 30. The authors note that total emissions from inventories can differ from measured fluxes but I think it is also important to note that the distribution of VOCs can be different due to unattributed sources. Karl et al (2018) shows that there is a large, unidentified source of oxygenated VOCs (OVOCs) in European cities that isn't properly represented in emission inventories. The same conclusions were drawn by McDonald et al. (2018), who showed that these sources likely result from solvent emissions due to the use of consumer and industrial products. As China places stricter restrictions on emissions, it's likely that the relative importance of different emissions sectors will also change. Could the authors provide some context here (as they do in other places in the manuscript), and perhaps provide a brief overview of the current VOC, NO_x, and CO distribution of China's emission inventory?

This section has been updated to provide some context about the sources of VOC emissions:

For example, previous studies have highlighted large discrepancies between emissions inventories and measured emissions for UK cities both for NO_x (Lee et al., 2015; Vaughan et al., 2016) and VOCs (Langford et al., 2010; Valach et al., 2015). Karl et al. (2018) revealed that non-methane VOC (NMVOC) emissions could be significantly higher than those used in most models by measuring emissions from Innsbruck, Austria. In addition to discrepancies in magnitude, the sources of emissions are not always correctly identified in inventories. Karl et al. (2018) indicates via emission measurements that a large, unidentified source of oxygenated VOCs is not represented in emissions inventories and that actual non-methane VOC (NMVOC) emissions could be significantly higher than those used in most models. As new emissions controls are introduced and emissions technologies improve the main sources of pollutant emissions will change. For example, McDonald et al. (2018) showed that an increasing proportion of the VOC emission budget is from volatile chemical products containing organic solvents (e.g. pesticides, cleaning agents and personal care products) as the transportation sector becomes cleaner. Inventories in China are associated with large uncertainties and are rapidly changing in response to economic development and new environmental regulations. Saikawa et al. (2017) reviewed and compared five different emissions inventories for China and found large disagreements between them. Thus, there is a critical need for reliable field measurements in order to further improve the emission estimates and reduce the uncertainty of inventories at local and regional scales (Zhao et al., 2017).

An inventory overview is given in Section 2.7 so was not thought to be appropriate here.

4. Section 2.3. How (and how frequently) were background PTR-MS measurements performed? The authors might consider referring to the instrument as a PTR-ToF-MS, since this is not a quadrupole instrument (the original PTR-MS). This distinction is important because the high time resolution of a PTR-ToF-MS is needed for flux calculations.

Zero air was sampled for 5 minutes each hour and these background mixing ratios were subtracted from ambient mixing ratios to give corrected mixing ratios. The following sentence has been added to the "VOC Sampling and Measurement" section:

The background signal was corrected for by sampling a zero air standard for 5 minutes every hour. Background mixing ratios were subtracted from measurement data to give corrected mixing ratios.

Any references to PTR-MS in the original manuscript have now been changed to PTR-ToF-MS.

5. Page 5, Line 30. “Despiked” is an odd term. Would “smoothed” be a better option?

The term “despiked” is commonly used within the flux community to refer to the process of removing erroneous, high-magnitude and often singular data points which are an artefact associated with high frequency data collection. Given its common use the authors believe it is an appropriate term to use in this instance.

6. Page 6, Line1: “allowing the software to calculate” is very vague. Was there an algorithm applied to the data to determine instrument lag in real time?

This section has been improved to make the lag determination process clearer. The workflow diagram included in response to reviewer 1 also makes this processing step clearer. The section now reads:

The lag time correction applied was determined by maximisation of the cross-covariance between pollutant concentration and the vertical wind component. When determining the lag time for each species a high-pass filter (Hartmann et al., 2018) is used which improves the precision of the determined lag time by an order of magnitude.

7. Page 6, Line 23. What do the authors mean by “non-stationary periods”? Does this mean that the flux changing too rapidly over the course of the averaging period? This statement seems repetitive with the previous sentence.

A non-stationary period is when the flux is variable over the averaging period to a degree that it no longer fulfils the fundamental simplifications of the conservation equation employed by the EC technique. Non-stationary periods hence do not permit conclusions about the actual surface emissions. This sentence has been removed as stationarity is defined and discussed in more in detail later in the manuscript in section 2.5.1 “Corrections and Filtering” and could be confusing for the reader if introduced here.

8. Figure 3. It is difficult to see the grey colored traces highlighting non-stationary periods, and it’s also confusing to have the contrasting periods also highlighted with grey. I would recommend adding markers for the points that were non-stationary, changing the color to clearly indicate these points, or simply remove these from the figure.

Figure 3, now figure 4, has been updated:

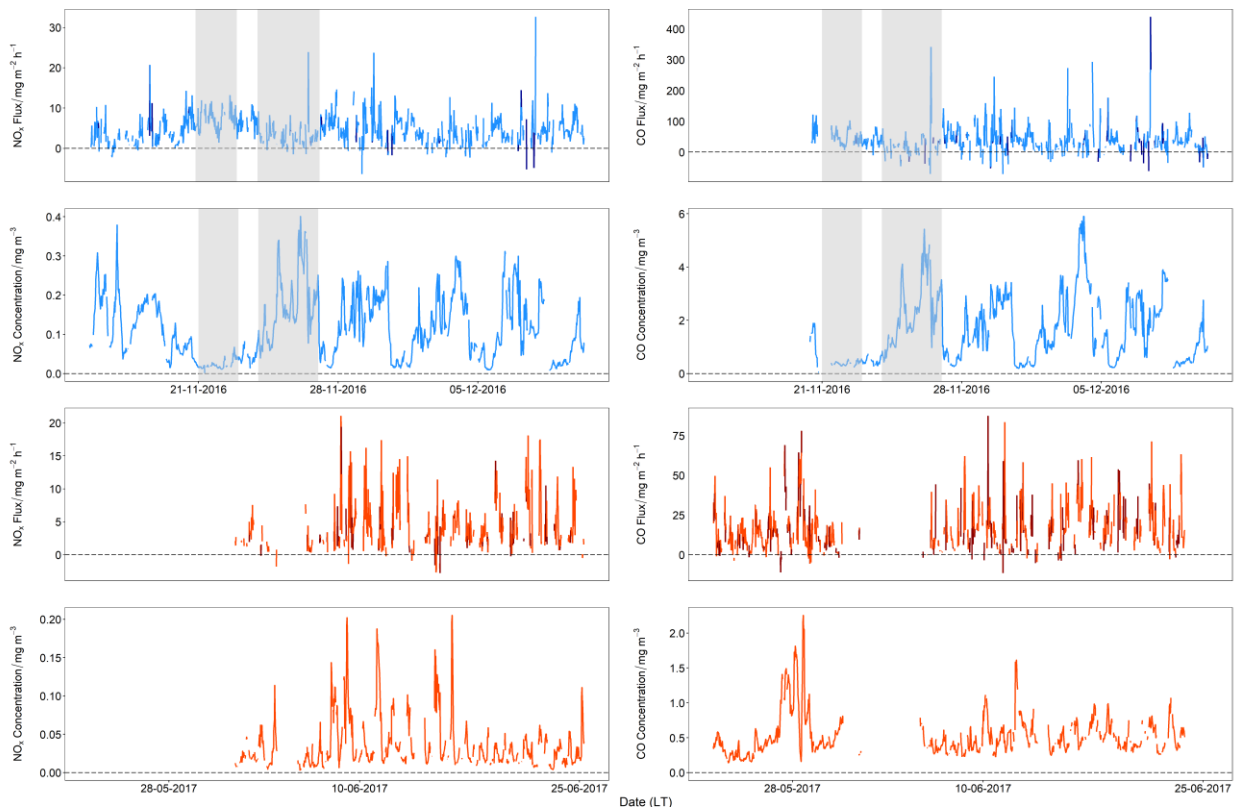


Figure 4: Time series data for 30 minute averaged NO_x and CO fluxes for the winter (blue trace) and summer (orange trace) campaigns with fluxes outside of the 60 % stationarity criteria shown in darker colours. Gaps in the time series are due to instrument problems. The two contrasting periods discussed in section 3.2 are highlighted in grey.

9. Page 13, Line 5 and Line 23. The authors mention that the major NO_x sources are likely the same between the two seasons, which is likely true for vehicle traffic. However, wintertime fluxes appear to be higher on average (~20%), and the wintertime diurnal patterns shows little resemblance to the summertime pattern (in line with the differences seen for CO). Furthermore, the nighttime flux of NO_x seems to be substantially higher in the winter. To my eye, this suggests that there are additional important NO_x sources, which are probably the same as those implicated for CO (i.e., residential heating). This seems to be supported by Fig 10, which shows that the Residential/Transportation ratio for NO_x is substantially larger in the winter than compared to summer.

The authors agree with this interpretation of the data and this was discussed to a degree in the following paragraph (page 13, lines 23 – 26 in original manuscript). The authors agree this could be made clearer for NO_x emissions however so have updated the following paragraph to:

The difference between the winter and summer diurnal averages was more significant for CO than for NO_x with larger CO emissions in the winter than the summer throughout the day. This may be in part due to an additional source unique to winter, for example domestic heating. Local heating sources are likely to be reasonably consistent throughout the day which may go some way to explaining why the relative difference between nighttime and daytime emissions is smaller than for NO_x . Local heating sources also appear to contribute to the NO_x emissions measured, albeit to a lesser degree than for CO. The rush hour peaks that were clearly observed in NO_x flux during the summer campaign are masked somewhat in the winter and the peak was broader in the evening which could be due to increased residential emissions throughout the day. ~~Given the similarity between the NO_x and CO diurnal variability, there is likely to be a traffic influence for CO. It is possible that additional emissions~~

from the residential sector were not the only reason for the difference in magnitude of winter and summer CO emissions however. Strong seasonal variability in the fluxes of CO has been observed for London as another megacity where CO emissions measured in summer were 69 % lower than in winter (Helfter et al., 2016). In this case, higher winter CO emissions were attributed mainly to vehicle cold starts and reduced fuel combustion efficiency due to colder ambient temperatures. It should be noted that this study took place in a temperate, developed city and Beijing needs more winter heating which until recently was primarily from coal. Indeed, Langford et al. (in prep.) identified signatures of coal and solid fuel combustion within the flux footprint of the measurement although residential heating is overwhelmingly dominated by district heating in this area of Beijing.

10. Page 13, Line 33. What is meant by “distant heating”? Is this heating using electricity?

This is a typo and should have read “district heating”, where heating is generated at centralised boilers and distributed to residential and commercial buildings. This has been changed.

11. Page 13, Lines 34 - Page 14, Line 6. The purpose of this paragraph isn’t entirely clear. Are the authors invoking HDV emissions to explain the higher CO and NO_x emissions during winter, or is this to explain the nighttime emissions during both seasons? Would one expect HDV’s to be more active during winter than during summer? It does appear that the summertime morning peak in NO_x, which is earlier than the CO peak, could be associated with the higher truck traffic before 06:00.

This was intended to give greater context to the vehicle fleet of Beijing, but the authors agree that clarity would be improved if this paragraph was integrated with an earlier paragraph (page 13, lines 5 – 22 in original manuscript).

As would be expected, peak traffic flow coincided with lowest average vehicle speeds and occurred at 08:00 and 18:00. NO_x emissions are dependent on fuel type, engine type, combustion temperature, vehicle speed, engine load and exhaust after-treatment technology. It is known that “stop - start” driving conditions and idling can enhance NO_x emissions compared to driving at steady speeds. Observations indicated that there are peaks in NO_x emissions during these rush hour periods. Beijing has attempted to reduce emissions through traffic management as well as by imposing emissions reduction regulations; for example yellow label vehicles, vehicles which do not meet the China I emissions standard have been forbidden from entering Beijing since 2014 (Yang et al., 2015). One management strategy imposed restrictions on heavy duty vehicles (HDVs) entering the city (past the sixth ring road) and only permits non-local vehicles to enter between 00:00 – 06:00. HDVs, particularly those using diesel fuel, are thought to be responsible for 85 % of NO_x emissions, whilst light duty vehicles (LDVs) are considered responsible for more than half of CO emissions (Yang et al., 2015). Some of the measured nighttime emissions of NO_x and CO could be attributed to HDVs making up a higher proportion of the vehicle fleet. CO emissions for summer also suggested a strong daytime traffic influence...

12. Figure 7: This figure is very nice. It is a little difficult to read the labels and to see the time axis on top of the darker colors of the fluxes. Could these be presented in larger fonts, and in bold?

Figure 7 (now figure 8) has been updated with larger text to make it clearer and easier to read:

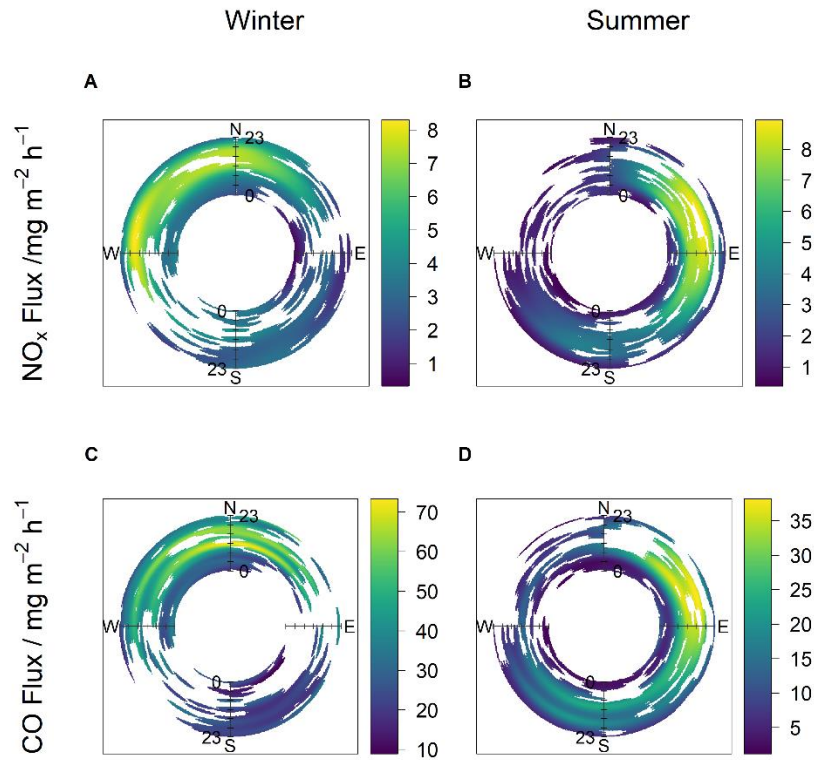


Figure 8. Polar annulus plots for NO_x and CO fluxes for both campaigns, showing the relationship between mean diurnal flux and wind direction. 0 – 23 refers to hour of day and the colour scale shows flux in $\text{mg m}^{-2} \text{h}^{-1}$.

13. Page 20, Line 30. When the authors mean that the change in B/T cannot be explained by temperature differences, I assume they mean atmospheric oxidation and not evaporation processes. This is clarified in the following sentence, but it would be good to be precise here since there is a lot of discussion about what could be affecting the B/T ratio (evaporation, chemistry, etc.) and mixing terms is a bit confusing.

This section has been updated to make this clearer:

*The difference in B/T concentration ratios does however indicate that VOC sources are changing between winter and summer as the change in ratio cannot be explained by **expected changes in atmospheric oxidation rates caused by seasonal differences in temperature**. Langford et al. (2009) points out that temperature can impact B/T ratios as reactivity rates increase with warmer temperatures but if temperature was driving the seasonal difference it would be expected that the B/T ratio measured during summer is higher than during winter.*

References

Hartmann, J., Gehrman, M., Kohnert, K., Metzger, S., and Sachs, T.: New calibration procedures for airborne turbulence measurements and accuracy of the methane fluxes during the AirMeth campaigns, *Atmos. Meas. Tech.*, **11**, 4567–4581, 2018.

Kljun, N., Calanca, P., Rotach, M. W., and Schmid, H. P.: A simple parameterisation for flux footprint predictions, *Bound.-Lay. Meteorol.*, **112**, 503–523, 2004.

Kljun, N., Calanca, P., Rotach, M. W., and Schmid, H. P.: A simple two-dimensional parameterisation for Flux Footprint Prediction (FFP), *Geosci. Model Dev.*, **8**, 3695–3713, 2015.

Heidbach, K., Schmid, H. P. and Mauder, M.: Experimental evaluation of flux footprint models, *Agr. Forest Meteorol.*, **246**, 142–153, 2017.

Metzger, S., Junkermann, W., Mauder, M., Beyrich, F., Butterbach-Bahl, K., Schmid, H. P., and Foken, T.: Eddy-covariance flux measurements with a weight-shift microlight aircraft, *Atmos. Meas. Tech.*, **5**, 1699–1717, 2012.

Heidbach, K., Analysis of Surface Energy Balance Measurements at the TERENO Station Graswang. Master's thesis, University of Munich, Germany, 2011.

Acton, W. J. F., Huang, Z., Davison, B., Drysdale, W. S., Fu, P., Hollaway, M., Langford, B., Lee, J., Liu, Y., Metzger, S., Mullinger, N., Nemitz, E., Reeves, C. E., Squires, F. A., Vaughan, A. R., Wang, X., Wang, Z., Wild, O., Zhang, Q., Zhang, Y., and Hewitt, C. N.: Surface–atmosphere fluxes of volatile organic compounds in Beijing, *Atmos. Chem. Phys. Discuss.*, 2020.

Measurements of traffic dominated pollutant emissions in a Chinese megacity.

Freya A. Squires¹, Eiko Nemitz², Ben Langford², Oliver Wild³, Will S. Drysdale^{1, 4}, W. Joe F. Acton³, Pingqing Fu^{5, 6}, C. Sue. B. Grimmond⁷, Jacqueline F. Hamilton¹, C. Nicholas Hewitt³, Michael Hollaway^{3, a}, Simone Kotthaus^{7, b}, James Lee^{1, 4}, Stefan Metzger^{8, 9}, Natchaya Pingintha-Durden⁸, Marvin Shaw¹, Adam R. Vaughan¹, Xinming Wang¹⁰, Ruili Wu¹¹, Qiang Zhang¹¹, and Yanli Zhang¹⁰

¹Wolfson Atmospheric Chemistry Laboratories, Department of Chemistry, University of York, York, YO10 5DD

²Centre for Ecology and Hydrology, Edinburgh, EH26 0QB

³Lancaster Environment Centre, Lancaster University, Lancaster, LA1 4YQ

⁴National Centre for Atmospheric Science, University of York, York, UK

⁵Institute of Atmospheric Physics, Chinese Academy of Sciences, Beijing, China

⁶Institute of Surface-Earth System Science, Tianjin University, Tianjin, China

⁷Department of Meteorology, University of Reading, Reading, UK

⁸National Ecological Observatory Network Program, Battelle, 1685 38th Street, Boulder, CO 80301, USA

⁹University of Wisconsin-Madison, Department of Atmospheric and Oceanic Sciences, 1225 West Dayton Street, Madison, WI 53706, USA

¹⁰Guangzhou Institute of Geochemistry, Chinese Academy of Sciences, Guangzhou 510640, China

¹¹Ministry of Education Key Laboratory for Earth System Modelling, Department of Earth System Science, Tsinghua University, Beijing, China

^aNow at: Centre for Ecology & Hydrology, Lancaster Environment Centre, Bailrigg, Lancaster, UK

^bNow at: Institut Pierre Simon Laplace, École Polytechnique, Palaiseau, France

Correspondence: James Lee (james.lee@york.ac.uk)

Abstract. Direct measurements of NO_x, CO and aromatic VOC (benzene, toluene, C₂-benzenes and C₃-benzenes) flux were made for a central area of Beijing using the eddy covariance technique. Measurements were made during two intensive field campaigns in central Beijing as part of the Air Pollution and Human Health (APHH) project, the first in November – December 2016 and the second during May – June 2017, to contrast winter and summertime emission rates. There was little difference in the magnitude of NO_x flux between the two seasons (mean NO_x flux was 4.41 ~~mg m⁻²~~ mg m⁻² h⁻¹ in the winter compared to 3.55 ~~mg m⁻²~~ mg m⁻² h⁻¹ in the summer). CO showed greater seasonal variation with mean CO flux in the winter campaign (34.7 ~~mg m⁻²~~ mg m⁻² h⁻¹) being over twice that of the summer campaign (15.2 ~~mg m⁻²~~ mg m⁻² h⁻¹). Larger emissions of aromatic VOCs in summer were attributed to increased evaporation due to higher temperatures. The largest fluxes in NO_x and CO generally occurred during the morning and evening rush hour periods indicating a major traffic source with high midday emissions of CO indicating an additional influence from cooking fuel. Measured NO_x and CO fluxes were then compared to the MEIC 2013 emissions inventory which was found to significantly overestimate emissions for this region, providing evidence that proxy-based emissions inventories have positive biases in urban centres. This first set of pollutant fluxes measured in

Beijing provides an important benchmark of emissions from the city which can help to inform and evaluate current emissions inventories.

1 Introduction

Rapid development and population growth has led to an ever increasing number of “megacities”, defined by the United Nations (UN) as a “metropolitan area with a total population of more than 10 million people” (United Nations’ Department Of Economic and Social Affairs: Population Division, 2016). In addition to being home to a large population, megacities are typically associated with high levels of industrialisation and extensive transportation networks making air pollution a common problem. Beijing is one such city that regularly experiences significant air quality problems. High levels of particulate matter (PM) in Beijing during winter months have been widely reported. In 2017, annual PM_{2.5} (PM with a diameter less than 2.5 μm) concentrations reached 58 $\mu\text{g m}^{-3}$, approximately six times greater than the World Health Organisation (WHO) guideline (Ministry of Ecology and Environment, the People’s Republic of China, 2018). During the summer, concentrations of ozone, O₃, a major component of photochemical smog, regularly exceeded the WHO 8-hour mean limit of 100 $\mu\text{g m}^{-3}$ in Beijing. Both PM and O₃ have detrimental impacts on public health and both are formed in the atmosphere from reactions by precursor emissions that include nitrogen oxides (NO_x), carbon monoxide (CO) and volatile organic compounds (VOCs). Secondary aerosols have been shown to comprise a large fraction of fine particulate matter in Beijing (Guo et al., 2014; Duan et al., 2020).

~~NO_x, the sum of nitrogen oxide (NO) and nitrogen dioxide (NO₂), and CO are two key anthropogenic pollutants. They are damaging to human health in their own right as well as forming secondary pollutants, PM and O₃.~~ China is the largest NO_x emitter globally and is estimated to contribute as much as 18 % ~~of to~~ global NO_x emissions (European Database For Global Atmospheric Research, 2000–2012) while Beijing itself is reported to have annual mean NO₂ concentrations 16 $\mu\text{g m}^{-3}$ higher than the national average (Ministry of Ecology and Environment, the People’s Republic of China, 2018). ~~In At~~ high concentrations, NO₂ is a respiratory irritant (Strand et al., 1998; Tunnicliffe et al., 1994). CO is a harmful air pollutant produced from incomplete combustion processes including those used in power generation and from vehicle engines. Liu et al. (2018) concluded that there is an association between short-term exposure to ambient CO and increased cardiovascular disease mortality, especially coronary heart disease mortality. For both these pollutants, traffic emissions tend to be the dominant source in megacities.

In order to manage air quality it is vital that legislators have a clear understanding of pollutant emissions to guide abatement strategies. Models of atmospheric chemistry provide an important mechanism to predict the efficacy of abatement measures on future air quality yet these predictions are only as certain as the emission inventories upon which they are based. For example, previous studies have highlighted large discrepancies between emissions inventories and measured emissions for UK cities both for NO_x (Lee et al., 2015; Vaughan et al., 2016) and VOCs (Langford et al., 2010; Valach et al., 2015). Karl et al. (2018) revealed that In addition to discrepancies in magnitude, the sources of emissions are not always correctly identified in inventories. Karl et al. (2018) indicates via emission measurements that a large, unidentified source of oxygenated VOCs is not represented in emissions inventories and that actual non-methane VOC (NMVOC) emissions could be signifi-

cantly higher than those used in most models ~~by measuring emissions from Innsbruck, Austria~~. As new emissions controls are introduced and emissions technologies improve the main sources of pollutant emissions will change. McDonald et al. (2018) showed that an increasing proportion of the VOC emission budget is from volatile chemical products containing organic solvents (e.g. pesticides, cleaning agents and personal care products) as the transportation sector becomes cleaner. Inventories in China are associated with large uncertainties and are rapidly changing in response to economic development and new environmental regulations. ~~Saikawa et al. (2017)~~ Saikawa et al. (2017) reviewed and compared five different emissions inventories for China and found large disagreements between them. Thus there is a critical need for reliable field measurements in order to further improve the emission estimates and reduce the uncertainty of inventories at local and regional scales (Zhao et al., 2017).

Given this pressing need for measurements of pollutant emissions, fluxes of NO_x, CO and commonly co-emitted VOCs (benzene, toluene, C₂-benzenes and C₃-benzenes) were calculated using the eddy-covariance (EC) technique for an urban area in Beijing. To the knowledge of the authors, this is the first time these emissions have been directly quantified in Beijing. This work was carried out as part of the Air Pollution and Human Health (APHH) Beijing project and an overview of this campaign can be found in Shi et al. (2019).

2 Methodology

2.1 Site Description

Measurements were taken from an inlet part-way up a 325 m meteorological tower at the Institute of Atmospheric Physics, Chinese Academy of Sciences (IAP, CAS) (39°58'28"N, 116°22'16"E) in central Beijing. The site is between the third and fourth ring roads and surrounding land use can be characterised as urban, being mainly residential with some busy (two and three lane dual-carriageway) roads nearby. The Jingzang Highway is approximately 400 m east of the site. Building heights surrounding the tower are predominantly 15 – 30 m in height, but with some almost 100 m tall within 500 m to the south of the tower. The site is in a 'green' area with some park space ~~with~~ and a canal close by. Measurements were made over two field campaigns; the winter campaign from 05 November 2016 – 11 December 2016 and the summer campaign from 22 May 2017 – 25 June 2017 to allow a seasonal comparison of emissions.

Instrumentation was housed in a temporary shipping container laboratory located at the base of the tower. Sample lines from an inlet platform at an elevation of 102 m ran down the tower to the laboratory. Air for sampling was drawn down a $\frac{1}{2}$ " O.D. (I.D. 9 mm) perfluoroalkoxy (PFA) tube at a rate of approximately 95 L min⁻¹ resulting in an inlet pressure of 44 kPa. This ensured turbulent flow was maintained (Reynolds Number \approx 7000) and attenuation of signals along the \sim 120 m sample line were minimised. Particles were removed from the airflow via a 90 mm Teflon filter mounted near the inlet which was changed at 24 hour intervals. The inlet of the tube comprised of a custom built, 32 mm diameter, stainless steel manifold cap with gauze to prevent larger debris entering the tube. The manifold was mounted 82 cm vertically below a sonic anemometer (Model HS-50, Gill Instruments) which measured the three wind vectors, u, v and w data at a rate of 10 Hz. During the winter campaign it was orientated NW from the tower and during the summer campaign towards the SE to measure the main wind

direction without obstructions. However, analysis of the turbulence characteristics did not suggest that the open structure of the tower affected the measurements even when the flow came through the tower. This may be due to the size of the eddy-motions at this measurement height.

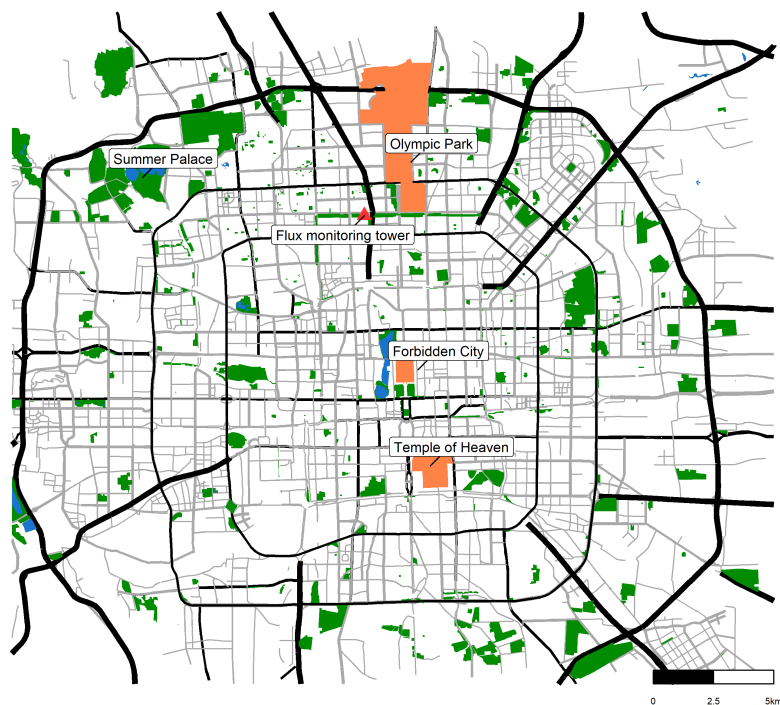


Figure 1. Measurement site position is shown by the red triangle between the third and fourth ring roads. Key landmarks of Beijing are highlighted in orange with major roads shown in black and smaller roads in grey. Parks are shown in green and water in blue. Surrounding land use is mainly residential with many restaurants within a few hundred meters of the site with the Jingzang Highway close by. Map was built using data from © OpenStreetMap contributors 2019. Distributed under a Creative Commons BY-SA License.

2.2 Instrumental Description

5 2.2.1 NO_x Sampling and Measurement

Concentrations of NO_x were measured using a dual-channel chemiluminescence instrument (Air Quality Designs Inc., Colorado). The instrument is similar to that described in Lee et al. (2009), but modified to enable high time resolution data to be collected with a residence time of 0.12 s inside the photolytic conversion cell. NO was measured directly by chemiluminescence from the reaction of NO and O₃ in one channel. The second channel measures total NO_x via photolytic conversion of

NO₂ to NO, at a wavelength of 395 nm, and then by chemiluminescence reaction with O₃, as per the direct measurement of NO. Instrument data were recorded at a frequency of 5 Hz.

The NO_x instrument was calibrated regularly (every 2 – 3 days) throughout the campaign using NO gas standards traceable to the UK's National Physical Laboratory's (NPL) NO scale. The instrument was calibrated via standard addition of a small flow of NO calibration gas to a flow of NO_x-free ambient air (NO_x was removed using a Sofnofil/charcoal trap). The sensitivities of the NO and NO_x channels were calculated by direct addition of the diluted NO calibration gas. The NO₂ – NO conversion efficiency within the NO_x channel was calculated by gas-phase titration of the diluted NO calibration gas with O₃ to create a known quantity of NO₂. During the calibration cycle, an instrument zero was quantified by diversion of sample flow to 'zero volumes' so that the chemiluminescence reaction was completed before the gas reached the detectors. Zero measurements were scheduled to occur for 15 seconds every hour through the normal operating schedule.

2.2.2 CO Sampling and Measurement

CO was measured using a resonance fluorescent instrument (Model AL5002, Aerolaser GmbH, Germany). Flows were adjusted to reduce cell lag times so data could be recorded at 5 Hz to match the NO_x data acquisition rate. Details of the unmodified system are described by ([Gerbig et al., 1996, 1999](#))[Gerbig et al. \(1996, 1999\)](#). The CO instrument was calibrated regularly (every 2 – 3 days) throughout the campaign as for the NO_x instrument using a 1 ppm CO in synthetic air standard. Previous urban flux measurements with this type of instrumentation have been presented for UK cities by ([Famulari et al., 2010](#); [Harrison et al., 2012](#); [Helfter et al. \(2010\)](#); [Harrison et al. \(2012\)](#); [Helfter et al. \(2016\)](#)).

2.3 VOC Sampling and Measurement

VOCs were measured using a Proton Transfer Reaction [Time-of-Flight](#) Mass Spectrometer (~~PTR-MS~~[PTR-ToF-MS](#)). The ~~PTR-MS~~ [PTR-ToF-MS](#) (PTR-MS 2000, Ionicon Analytik, Innsbruck, Austria) was installed at the base of the tower and ~~subsampling~~ [sampled](#) from the common inlet line at 30 sccm. The instrument was operated with a 5 Hz measurement frequency. The drift tube maintained at 60 °C, with a pressure of 1.9 mbar and 490 V applied across it. This gave an E/N (the ratio between electric field strength and buffer gas density) of 120 Td in the drift tube. This set up is described in more detail by ~~Acton et al. (in prep.)~~ [Acton et al. \(2020\)](#).

The ~~PTR-MS~~ [PTR-ToF-MS](#) was calibrated twice a week during both the winter and summer campaigns using a VOC standard containing methanol, acetonitrile, ethanol, 1,3-butadiene, acetone, isoprene, butenone, butan-2-one, benzene, toluene, m-xylene and 1,2,4-trimethylbenzene at 1 ppmv (National Physics Laboratory, Teddington, UK). The standard was dynamically diluted in zero air to provide a six point calibration. In the winter campaign the instrument ~~also was~~ [was also](#) calibrated using two Ionicon standards the first containing methanol, acetonitrile, acetaldehyde, ethanol, acrolein, acetone, isoprene, crotonaldehyde, butan-2-one, benzene, toluene, o-xylene, chlorobenzene, α -pinene and 1,2-dichlorobenzene at 1 ppmv each and the second made up of formaldehyde, acetaldehyde, acrolein, propanal, crotonaldehyde, butanal, pentanal, hexanal, heptanal and octanal at 1 ppmv, nonanal at 600 ppbv and decanal at 500 ppbv. ~~PTR-MS data~~ [The background signal was corrected for](#)

by sampling a zero air standard for 5 minutes every hour. Background mixing ratios were subtracted from measurement data to give corrected mixing ratios. PTR-ToF-MS data was processed using PTRViewer (Ionicon Analytik).

2.4 Data Processing

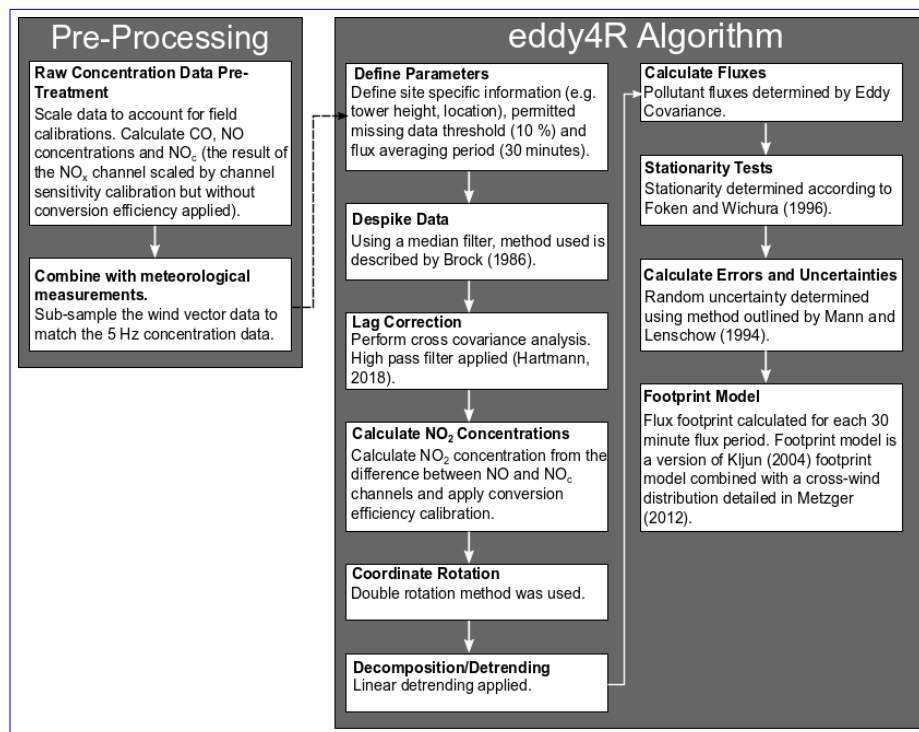


Figure 2. Workflow schematic summarising the data processing steps required for calculation of NO_x and CO fluxes.

Prior to the calculation of pollutant fluxes, the raw data were scaled to take account of calibrations. The sensitivity within each channel of the NO_x chemiluminescence instrument remained consistent throughout the winter and summer campaigns so data were scaled using median sensitivity values. The conversion efficiency of the NO₂-NO_x channel gradually deteriorated over the two campaigns and so NO₂ data were scaled using linearly interpolated conversion efficiency values. As highlighted in Fig. 2, the NO₂ calibration was applied in two stages, the first during pre-processing and the second following lag correction. During the pre-processing stage the channel sensitivities (counts pptv⁻¹) determined by field calibration are applied to both the NO and NO_x channels to give NO (pptv) and a term referred to as converted NO_x channel counts 'NO_c'. NO₂ is then calculated from the difference between the time-lagged corrected NO_c and NO divided by conversion efficiency. The time lag correction is described below. For CO concentration data, the instrument sensitivity following each calibration was directly applied and the sensitivity remained consistent for the duration of the two campaigns.

Concentration data were coupled with wind data reported by the sonic anemometer by sub-sampling the wind vector data to match the 5 Hz concentration data. Data were then despiked prior to flux calculation as per the method described in Brock

(1986) and Starkenburg et al. (2016). Following despiking, the lag time between vertical wind velocity measured in-situ on the tower and the pollutant concentrations, measured on the ground, was calculated. The lag time correction ~~applied~~ was determined by ~~first allowing the software to calculate the optimum lag for each averaging period by~~ maximisation of the cross-covariance between ~~concentration and pollutant concentration and the~~ vertical wind component. ~~Because there was no discernible pattern or trend in the lag-times and to prevent the flux bias that cross-covariance maximisation can introduce when fluxes are small (Langford et al., 2015), the final fluxes were calculated by applying the median time-lag value for each campaign to all flux periods~~ When determining the lag time for each species a high-pass filter (Hartmann et al., 2018) was used which improves the precision of the determined lag time by an order of magnitude. The median lag time was then calculated for each species during each campaign. The lag time between the concentration and vertical wind speed during the winter campaign was found to be ~~9.6 s, 10.0 s, 10.2~~ 9.6 ± 0.4 s, 10.0 ± 0.4 s, 10.2 ± 0.3 s for NO, NO₂ and CO respectively. For the summer campaign lag times were calculated as ~~9.4 s, 9.8 s and 10.6 s~~ 9.4 ± 0.4 s, 9.8 ± 0.3 s and 10.6 ± 0.5 s. ~~Because there was no discernible pattern or trend in the lag-times and to prevent the flux bias that cross-covariance maximisation can introduce when fluxes are small (Langford et al., 2015), the final fluxes were calculated by applying the median time-lag value for each campaign to all flux periods.~~ Lag time correction was performed using the same method for the PTR-MS PTR-ToF-MS VOC concentrations. Lag times were calculated for isoprene (summer data) and benzene (winter data) within a 5 – 15 s window and these values were then applied to all compounds. Where the lag time was found to be outside of the 5 – 15 s range a standard lag time of 9 s was applied.

2.5 Flux Calculations

The flux, F , of each species, which can be defined as the vertical transport of a pollutant per unit area per unit time, was then calculated using the eddy covariance (EC) method (Lee et al., 2004):

$$F \approx \overline{w'c'} \quad (1)$$

where w' is instantaneous change in vertical wind speed (i.e. $w' = w - \bar{w}$, where overbars denote averages) and c' is instantaneous change in pollutant concentration. The flux was calculated over a 30 minute averaging period and quantified using the eddy4R family of R-packages (Metzger et al., 2017) with a customized eddy-covariance workflow template to suit the requirements of ~~our study~~ this study. Figure 2 shows the key steps involved in the calculation of pollutant fluxes. Random uncertainty was calculated using the method outlined by Mann and Lenschow (1994). The flux limit of detection was taken to be twice the random error. It should be noted that, due to the high measurement height, 30 minute fluxes might be an underestimation of the 'true' flux as the averaging period may not capture low frequency contributions. To quantify the effect, a comparison between 30 minute, 60 minute and 120 minute averaging intervals was carried out for a week-long period of the summer campaign which indicated 30 minute fluxes were 93 % of the 60 minute fluxes whilst 120 minutes fluxes were considered too long an averaging periods for sufficient temporal resolution. Additionally increasing the length of averaging time introduces more non-stationary periods into the data. The 30 minute flux is therefore a compromise between capturing the entirety of the flux by keeping the low frequency flux loss small (7 %) and having sufficient temporal resolution to relate the measurements

to real-world processes. Fluctuations in temperature and humidity can impact fluxes by causing variation in air density (Webb et al., 1980). For closed path systems, such as those used in this study, air density variations caused by sensible-heat flux are negligible however variations due to latent heat flux may need to be corrected for. For CO fluxes, samples were passed through a dryer negating the need for this correction, however latent heat flux could have an impact on the NO_x fluxes (Moravek et al., 2019). The magnitude of the correction is proportional to the concentration/flux ratio which for reactive species, like NO_x, is small. The effect of latent heat flux on NO_x fluxes was found to be significantly less than 1 % throughout the campaigns and so the WPL correction was not applied (Pattey et al., 1992). The effect of high-frequency spectral loss on NO_x and CO fluxes was investigated using a wavelet-based methodology (Nordbo and Katul, 2013). Spectral losses were found to be less than 3 % and so were not corrected for.

10 2.5.1 Corrections and Filtering

There are numerous assumptions made when calculating EC fluxes, all of which can introduce uncertainties in the derived quantity. Further conditions need to be met for the measured flux to be representative of surface flux. Assumptions include but are not limited to, the flux being fully turbulent with all transport done by eddy transfer, the terrain being homogeneous, measurements being made within the boundary layer, air density fluctuations being negligible and conditions remaining stationary.

15 A common method to deal with periods of low turbulence, during which the flux at the measurement height may not reflect the surface flux, is to filter the data based on a friction velocity (u_*) threshold. Friction velocity accounts for shear stress in the turbulent boundary layer, and can be calculated from the instantaneous wind vectors u' , v' and w' (Foken, 2017). Concepts for u_* filtering were originally developed by the community measuring CO₂ exchange with vegetation. Here, incorrect application of u_* filtering can lead to a “double-counting” of flux as described in Aubinet (2008). In addition, by filtering out low-turbulence cases (low u_* values) the data set can become biased with little information about nighttime and winter periods. Whilst for CO₂ exchange with vegetation fairly robust parametrisations exist that can be used to gap-fill periods of low turbulence, no such information is yet available for urban fluxes. Liu et al. (2012) therefore argue against applying u_* filtering for the IAP site during a similar analysis of CO₂ fluxes, and suggest more errors could be introduced through filtering than not. Thus u_* filtering was also not applied to the data presented here, unless otherwise stated. Approximately 29 % of winter fluxes and 11 % of summer fluxes ~~are were~~ associated with u_* values below 0.175 m s⁻¹. Average fluxes as a function of u_* values are presented in ~~figFig~~ A1 and the effect of u_* filtering on diurnal variation is shown in ~~figFig~~ A2. These show the maximum possible effect of low turbulence on fluxes. Because low turbulence is correlated with nighttime conditions during which emission activity is reduced, an increasingly stringent u_* filter preferentially removes periods during which the surface flux is smaller than the average. This may result in an increase in the average nighttime flux that does not necessarily reflect suppression of the flux by

20
25
30 lack of turbulence.

Stationarity is another important consideration for flux data. Stationarity is when the flux is statistically invariant over the averaging period and is quantified using the method described in Foken and Wichura (1996). The stationarity criterion is likely not to be met when fluxes are small and subject to a large random uncertainty; this is irrespective of whether the conditions are actually non-stationary. As a result this filter tends to remove the smallest fluxes and can bias flux results (e.g. Nemitz

et al., 2018). A broad stationarity filter of 60 % was applied to all flux data presented in any average diurnals, though non-stationary data is presented and highlighted in time series plots. This stationarity filter was used as a more rigorous filter of 30 %, commonly used within the CO₂ flux community, removed a large proportion of the data. During the winter campaign 23 % of NO_x fluxes and 22 % of CO fluxes were non-stationary under this more rigorous criterion. During the summer
5 campaign these proportions were 16 % of NO_x fluxes and 39 % of CO fluxes. The 60 % threshold used was determined to be appropriate as it falls within the stationarity range recommended for “general use”, such as using diurnal averages to interpret trends (Foken et al., 2004). Further to these corrections, any periods where the boundary layer was within 30 m ~~of~~ above the measurement height were removed from the data. Boundary layer height was measured throughout both campaigns using a
10 celimeter (Vaisala CL31). The data are analysed using the CABAM algorithm (Kotthaus and Grimmond, 2018).

It was also important to consider storage effects; due to the build-up or dilution of the pollutants below the measurement height. Build-up can occur during periods of low turbulence e.g. during the night and this accumulation reduces the flux at the measurement height with respect to the emission at the ground (Finnigan, 2006). As conditions become more turbulent the accumulated pollutant ~~concentrations gets diluted~~ concentration gets diluted again and the measured flux contains a component that originates from the stored material rather than emission. Gas concentration profile measurements can be used
15 to allow detection of build-ups by providing data for computing a storage term below measurement height. In this case, the storage flux, F_s , at time, t , was calculated according to the following equation (Andreae and Schimel, 1990):

$$F_s(t) = \frac{C_{(t-\frac{t}{2})} - C_{(t-\frac{t}{2})}}{t} \quad (2)$$

The validity of calculating the storage flux at a single measurement height was evaluated by comparing CO₂ concentration measurements made at the measurement height and CO₂ concentration profile measurements made at three different heights
20 on the tower. By comparing the evolution of the CO₂ concentration at the single measurement height with ~~that measured at three heights up the tower~~ tower for CO₂ the CO₂ profile measurements, it was determined that calculating storage flux using the single concentration at the measurement height was a reasonable approximation of the storage within the column. It should be noted that this storage correction to some extent takes care of the flux suppression at low turbulence, except for the interaction with advection and chemistry.

Throughout, this paper focusses on the analysis of total NO_x flux rather than NO and NO₂ flux separately. Whilst the two compounds undergo rapid interconversion the total should be conserved at the time-scale that governs the transport from the surface to the measurement height; the major loss route for NO_x is HNO₃ formation through reaction with the hydroxyl (OH) radical. This loss is assumed to be negligible between ground emission and sampling at the tower inlet. Calculation of Deardorff velocity suggests that on average the time taken for a parcel of air to reach the 102 m measurement point is ~68 s (Deardorff,
30 1970). Assuming average OH concentrations of 1×10^6 molecules cm⁻³ it is estimated that less than 1 % reacts with OH at this time-scale.

2.6 Footprint Model

A flux footprint is the area surrounding the measurement tower that contributes to a measured flux based on factors such as wind speed, wind direction, atmospheric stability and surface roughness. A statistical flux footprint model can be used to quantify the flux contribution of each cell of an emission grid relative to the distance away from the measurement position in all directions, creating a weighing matrix that estimates the ground influence of a particular cell contributing to the observed emission flux. A footprint was calculated for each half hour flux period at 100 m resolution. The footprint model used is ~~described in detail in Kljun et al. (2004) and based on Kljun et al. (2004) with a cross-wind distribution detailed in~~ Metzger et al. (2012). Surface roughness values were taken from Liu et al. (2012) and taken to be 2.5 m, 3.0 m, 5.3 m and 2.8 m for the NE, SE, SW, and NW wind quadrants respectively. Figure 3 shows the average footprint for the winter and summer campaigns with the 30 %, 60 % and 90 % cumulative contributions to the measured flux represented by the contours.

For both campaigns the 90 % contribution to the measured flux extended as far as 7 km from the measurement site for some averaging periods, however, as shown in ~~fig~~Fig. 3 on average 90 % of the contribution to measured emissions was from within 2 km of the tower. Figure 3 shows the difference in areas of influence covered during the winter and summer campaigns due to differences in dominant wind directions. During the winter, the measured fluxes were predominantly from the north-west encompassing Beitucheng West Road and a block of predominantly commercial buildings and restaurants. The mean footprint maxima, the distance away from the tower at which the maximum contribution to the measured flux occurs, falls 0.26 km away from the tower in winter. In summer, the fluxes were mostly influenced by areas to the north east and east of the tower, encompassing the Jingzang Expressway. The mean footprint maxima for summer was also 0.26 km away from the site.

2.7 Inventory

The measured pollutant fluxes were compared with the Multi-resolution Emissions Inventory for China (MEIC, ~~Qi et al. (2017);~~ Qi et al. (2017), <http://www.meicmodel.org/>, last access: 19 May 2020) to evaluate how well the inventory describes the diurnal evolution of pollutants and their absolute magnitude. MEIC emissions are available at 0.25×0.25 degree resolution and were downscaled to 3×3 km resolution on a sector by sector basis following the approach of Zheng et al. (2017). MEIC considers five emission source sectors; power plants, industry, transport, residential, and agricultural ~~and is presented at a resolution of 3 km^2 .~~ Agricultural emissions are not relevant within our flux footprint so were not included in this work. Emissions are available on a monthly basis, and are assumed to be the same each day of the month, and a diurnal cycle appropriate to Chinese sources is applied to each emission sector. Example emissions for Beijing are presented in Fig. A3 for November. The NO_x and CO emission predicted by the inventory are calculated from the multiplication of each footprint matrix by the MEIC grid. ~~For this evaluation, an optimised version of the MEIC v1.3 inventory for 2013 was used that was derived by fitting the NAQPMS model with observed pollutant concentrations during the campaign periods (Du et al., 2019). Temporal variability is represented in the inventory with twelve emissions grids, one for each calendar month. The emissions throughout the month are assumed to be the same each day with a diurnal cycle imposed. Example emissions grid for Beijing are presented in figure A3 for November.~~



Figure 3. The mean flux footprints for the winter and summer campaigns. The site is shown by the red triangle in the centre of the map. Each square is 100 m^2 and the brighter colours indicate a greater influence on measured emission for a particular area. The white rings show the areas contributing 30 %, 60 % and 90 % to the flux total with inner ring representing the 30 % contribution and outer ring representing 90 % contribution. The 90 % of the influence from the footprint extends up to 2 km away from the tower with maximum contribution 0.26 km away from the tower. Map was built using data from © OpenStreetMap contributors 2019. Distributed under a Creative Commons BY-SA License.

In order to match the scales of the footprint matrix and the inventory, a pseudo $100 \text{ m} \times 100 \text{ m}$ MEIC grid was created by splitting the 3 km resolution inventory into smaller $100 \text{ m} \times 100 \text{ m}$ grid squares, each with the same emission value.

3 Results & Discussion

Statistics for NO_x and CO fluxes and concentrations presented in this work are shown in [table-Table 1](#). Figure 4 shows a time series of measured NO_x and CO fluxes during the winter and summer measurement campaigns where grey coloured traces highlight data which does not meet the 60 % stationarity criteria. For winter, 3.5 % of NO_x fluxes and 8.2 % of CO fluxes were non-stationary. In summer, slightly fewer measurements did not meet the stationarity criteria with 3.1 % of NO_x fluxes and 7.3 % of CO fluxes falling outside the 60 % stationarity limits. The mean flux for NO_x during the winter measurement period was $4.4 \pm 3.9 \text{ mg m}^{-2} \text{ h}^{-1}$ and $3.6 \pm 3.7 \text{ mg m}^{-2} \text{ h}^{-1}$ for the summer measurement period. For CO, there was a larger difference between the two seasons with the mean flux calculated as $35 \pm 40 \text{ mg m}^{-2} \text{ h}^{-1}$ for winter and $15 \pm 14 \text{ mg m}^{-2} \text{ h}^{-1}$ in summer. Some of the calculated fluxes ~~are~~ were negative, corresponding to deposition to the surface, however, as expected in an urban environment, the net flux ~~is~~ was strongly positive indicating emission. The average NO_x fluxes for the winter and summer periods ~~are~~ were similar suggesting an emission source that ~~does~~ did not change much between seasons. In contrast the average CO flux ~~is~~ was over double in the winter compared to the summer indicating an additional source in the winter.

Table 1. Summary table for NO_x and CO fluxes and concentrations. Data presented is for fluxes which are within 60 % stationarity criteria for all u_* values.

	Winter		Summer	
Concentration (mg m ⁻³)	NO _x	CO	NO _x	CO
Mean	0.103	1.41	0.0310	0.502
Median	0.0839	1.01	0.0213	0.429
Percentiles				
5th	0.0154	0.268	0.00810	0.210
95th	0.252	3.60	0.0876	0.998
Standard Deviation	0.0776	1.16	0.0278	0.267
Flux (mg m ⁻² h ⁻¹)				
Mean	4.41	34.7	3.55	15.2
Median	4.14	32.0	2.45	12.4
Percentiles				
5th	-1.24	-27.0	-0.0139	-2.15
95th	10.6	103	11.5	42.9
Standard Deviation	3.86	40.1	3.69	14.4

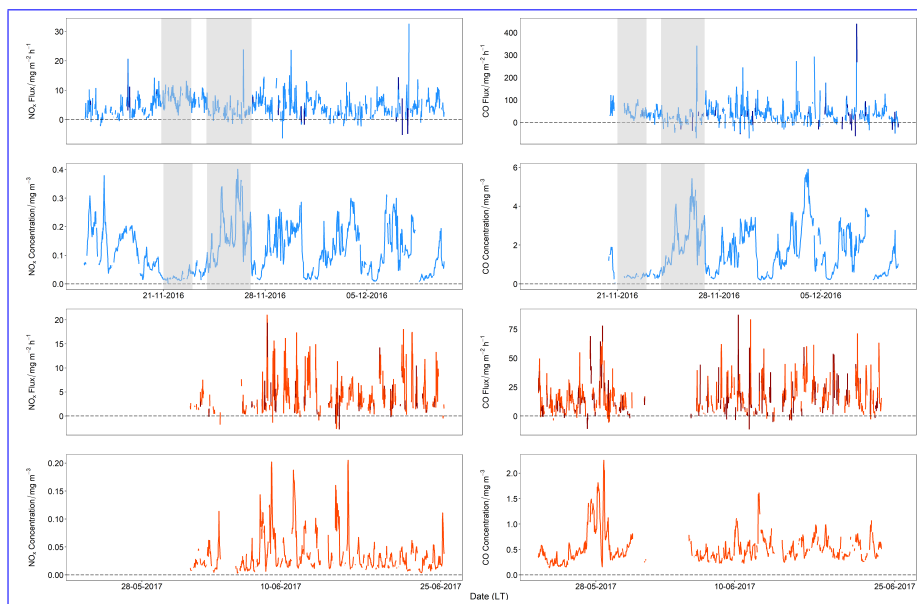


Figure 4. Time series data for 30 minute averaged NO_x and CO fluxes for the **summer and winter campaign**; the (blue trace corresponds to measurements taken during the winter campaign) and the orange the summer campaign. Grey coloured flux traces correspond to (orange trace) campaigns with fluxes outside of the 60 % stationarity criteria shown in darker colours. Gaps in the time series are due to instrument problems. The grey boxes on the winter timeseries plots highlight two contrasting periods discussed in section 3.2 are highlighted in grey.

When considering previous literature, the NO_x fluxes measured in Beijing were low compared to London, UK where net emissions were in the range of 10.8 $\text{mg m}^{-2} \text{ h}^{-1}$ – 14.4 $\text{mg m}^{-2} \text{ h}^{-1}$ (Lee et al., 2015). A study investigating NO_x fluxes across 13 urban locations in Norfolk, Virginia reported values in the range of 18 – 28 $\text{mg m}^{-2} \text{ h}^{-1}$, up to 8 times higher than those measured in Beijing (Marr et al., 2013). Fluxes measured in Beijing were similar to those measured in Innsbruck at a roadside site in July – October, 2015 where NO_x fluxes of 2.5 – 5.2 $\text{mg m}^{-2} \text{ h}^{-1}$ were reported (Karl et al., 2017). For CO, measured fluxes in central London were 2 – 3 times lower than those measured in Beijing. Average winter (December – February) CO flux was reported to be $12.5 \pm 3.4 \text{ mg m}^{-2} \text{ h}^{-1}$ and average summer (June – July) CO flux was reported to be $4.0 \pm 0.1 \text{ mg m}^{-2} \text{ h}^{-1}$, for the measurement period September 2011 – December 2014 (Helfter et al., 2016). NO_x emissions are likely to be lower in Beijing than for other cities as the majority of ~~onroad-road~~ vehicles in Beijing are light-duty gasoline vehicles (LDGVs) which made up to 93 % of the vehicle fleet in Beijing in 2013 (Yang et al., 2015) compared to other cities which have a higher proportion of diesel vehicles. However, because fluxes vary spatially within each city, care needs to be taken when comparing measurement datasets as the type of the location within the city needs to be considered.

3.1 Average diurnal cycles

Figure 5 shows the mean diurnal profile for both campaigns for pollutant fluxes, concentrations and ~~mixing-mixed~~ layer height. Diurnal profiles are a useful way to visualise flux data, as time of day may indicate processes responsible for emissions. During the winter campaign, the NO_x fluxes were lower during the early hours of the morning (between 00:00 – 05:00) ranging between 1.9 $\text{mg m}^{-2} \text{ h}^{-1}$ and 3.6 $\text{mg m}^{-2} \text{ h}^{-1}$. After 06:00, the NO_x fluxes increased and remained elevated, though variable, throughout the day with a mean daytime value (06:00 – 18:00) of 5.1 $\text{mg m}^{-2} \text{ h}^{-1}$. The NO_x fluxes decreased again in the evening. The daily variability in CO fluxes followed a similar pattern to NO_x. The mean daytime CO flux was 38 $\text{mg m}^{-2} \text{ h}^{-1}$, and was lower during the night (19:00 – 05:00) with a mean nighttime value of 29 $\text{mg m}^{-2} \text{ h}^{-1}$. Concentrations are influenced by meteorology and long range transport as well as local emissions (in this study local emissions refer to emissions from within the flux footprint). NO_x and CO concentrations remained constant during the night due to stability in the ~~mixing-mixed~~ layer height. When NO_x and CO emissions increased after 05:00, this enhancement in flux was reflected in the concentration data with a small peak in NO_x and CO concentrations around 06:00, though the effect is masked as the ~~mixing-mixed~~ layer height begins to increase. Concentrations decreased to their minima at 15:00 when the ~~mixing-mixed~~ layer height reached its highest point and increase again when the ~~mixing-mixed~~ layer height contracted over night.

~~For Fluxes were lower during~~ the summer campaign, ~~fluxes are slightly lower~~ than during the winter. The mean nighttime flux was less than 1.6 $\text{mg m}^{-2} \text{ h}^{-1}$ for NO_x and 6.5 $\text{mg m}^{-2} \text{ h}^{-1}$ for CO. Emissions rapidly increased after 05:00 and started to decrease at around 17:00. Daytime emissions for NO_x were fairly consistent with a mean value of 4.6 $\text{mg m}^{-2} \text{ h}^{-1}$. The first of two distinct peaks in the observed NO_x fluxes occurred at 07:00, where emissions reached 5.4 $\text{mg m}^{-2} \text{ h}^{-1}$ and the second occurred at 17:00 with a slightly higher value of 6.3 $\text{mg m}^{-2} \text{ h}^{-1}$. The daytime profile for CO showed two distinct peaks in emissions; the first peak occurred at 11:00 with CO emissions around 30 $\text{mg m}^{-2} \text{ h}^{-1}$

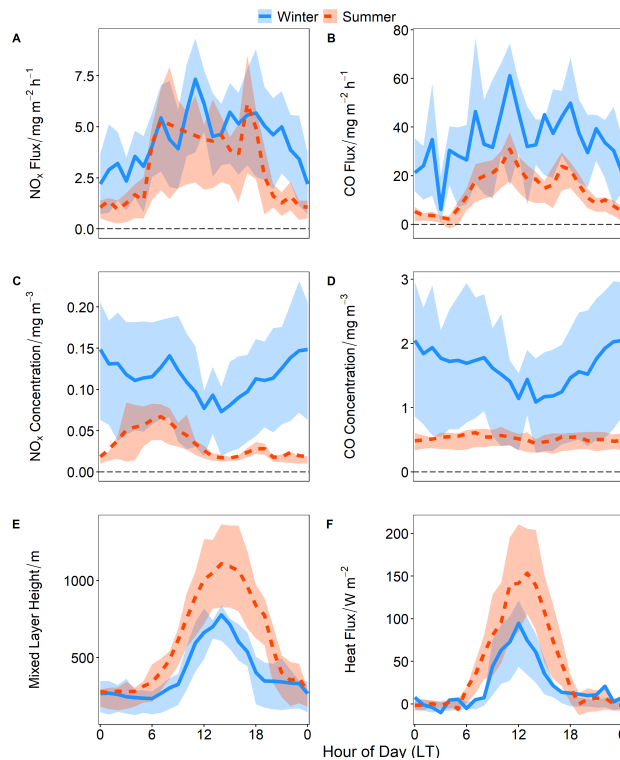


Figure 5. Average diurnal profiles for A) NO_x flux, B) CO flux, C) NO_x concentration, D) CO concentration and E) mixing-mixed layer height and F) heat flux. Blue, solid lines are for measurements taken during the winter campaign and the orange, dashed lines are measurements taken during the summer campaign. The shaded areas represent the 25th and 75th percentiles to show the spread of the data. For the NO_x and CO fluxes, only stationary data has been used but no u_* filtering has been applied when doing the diurnal averaging, as described in section 2.5.1.

and the second at 17:00, when CO fluxes were around $24 \text{ mg m}^{-2} \text{ h}^{-1}$. Between these times the CO emissions dipped with a minimum daytime value of $16 \text{ mg m}^{-2} \text{ h}^{-1}$ at 14:00 – 15:00. The influence of local emissions on concentration is more clearly observed during the summer campaign; the peaks in NO_x and CO fluxes at 17:00 occurred at the same time as an enhancement in NO_x and CO concentration. Both NO_x and CO concentrations reached their daytime minima at 14:00 - 15:00 when the mixing-mixed layer height was at its peak.

Given that the NO_x emissions were fairly consistent between the two seasons it is likely that the major sources of NO_x do not vary significantly over the year. In urban areas, vehicular emissions tend to be a dominant source of NO_x (Parrish et al., 2009; von Schneidmesser et al., 2010; Borbon et al., 2013) and previous studies measuring NO_x fluxes have attributed emissions to vehicles (Lee et al., 2015; Vaughan et al., 2016). Diurnal variation in summer NO_x emissions agree well with previously reported diurnal variation in Beijing's traffic flow. Jing et al. (2016) show that traffic flow (vehicle number per hour) begins to increase from 05:00 in the morning, corresponding to the observed increase in NO_x emissions. As would be expected, peak

traffic flow coincided with lowest average vehicle speeds and occurred at 08:00 and 18:00. NO_x emissions are dependent on fuel type, engine type, combustion temperature, vehicle speed, engine load and exhaust after-treatment technology. It is known that “stop - start” driving conditions and idling can enhance NO_x emissions compared to driving at steady speeds. ~~Observations and observations~~ indicated that there are peaks in NO_x emissions during these rush hour periods. ~~CO-emissions-Beijing has attempted to reduce emissions through traffic management as well as by imposing emissions reduction regulations; for example yellow label vehicles, vehicles which do not meet the China I emissions standard have been forbidden from entering Beijing since 2014 (Yang et al., 2015). One management strategy imposed restrictions on heavy duty vehicles (HDVs) entering the city (past the sixth ring road) and only permits non-local vehicles to enter between 00:00 – 06:00. HDVs, particularly those using diesel fuel, are thought to be responsible for 85 % of NO_x emissions, whilst light duty vehicles (LDVs) are considered responsible for more than half of CO emissions (Yang et al., 2015). Nighttime emissions of NO_x and CO during both seasons could be attributed to HDVs making up an unusually high proportion of the vehicle fleet. CO emissions~~ for summer also suggested a strong daytime traffic influence, although the peak at 11:00 may indicate an additional source, possibly relating to cooking given the time of day. Cooking was identified as a major contributor to the organic PM₁ flux in aerosol flux measurements made during the same measurement period (Langford et al., *in prep.*). NO_x and CO fluxes measured during the winter also indicated some traffic influence, although the trend is less clearly resolved than for the summer measurements. Winter NO_x emissions had a peak of $6.0 \text{ mg m}^{-2} \text{ mg m}^{-2} \text{ h}^{-1}$ at 07:00 and there was a broader evening peak of similar magnitude between 17:00 – 18:00. NO_x flux peaked at 11:00 at $6.7 \text{ mg m}^{-2} \text{ mg m}^{-2} \text{ h}^{-1}$. CO flux was more variable; there was a small peak around the time of the morning rush hour though this was not as clearly resolved as it is for NO_x. CO flux peaked at 11:00 and in the evening though the profile showed greater short term variability for NO_x.

The difference between the winter and summer diurnal averages was more significant for CO than for NO_x with larger CO emissions in the winter than the summer throughout the day. This may be in part due to an additional source unique to winter, for example domestic heating. Local heating sources are likely to be reasonably consistent throughout the day which may go some way to explaining why the relative difference between nighttime and daytime emissions is smaller than for NO_x. ~~Given the similarity between the NO_x and CO diurnal variability, there is likely to be a traffic influence~~ Local heating sources also appear to contribute to the NO_x emissions measured, albeit to a lesser degree than for CO. The rush hour peaks that were clearly observed in NO_x flux during the summer campaign are masked somewhat in the winter and the peak was broader in the evening which could be due to increased residential emissions throughout the day. It is possible that additional emissions from the residential sector were not the only reason for the difference in magnitude of winter and summer CO emissions however. Strong seasonal variability in the fluxes of CO has been observed for London as another megacity where CO emissions measured in summer were 69 % lower than in winter (Helfter et al., 2016). In this case, higher winter CO emissions were attributed mainly to vehicle cold starts and reduced fuel combustion efficiency due to colder ambient temperatures. It should be noted that this study took place in a temperate, developed city and Beijing needs more winter heating which until recently, was primarily from coal. Indeed, Langford et al., (*in prep.*) identified signatures of coal and solid fuel combustion within the flux footprint of the measurement although residential heating is overwhelmingly dominated by distance-district heating in this area of Beijing. ~~Beijing has attempted to reduce emissions through traffic management as well as by imposing emissions~~

reduction regulations; congestion reduces vehicle speed which can increase emissions (Yang et al., 2015). One management strategy imposed restrictions on heavy duty vehicles (HDVs) entering the city (past the sixth ring road) and only permits non-local vehicles to enter between 00:00–06:00. HDVs, particularly those using diesel fuel, are thought to be responsible for 85 % of NO_x emissions, whilst light duty vehicles (LDVs) are considered responsible for more than half of CO emissions (Yang et al., 2015). Nighttime emissions of NO_x and CO could be attributed to HDVs making up an unusually high proportion of the vehicle fleet. Yellow label vehicles, vehicles which do not meet the China I emissions standard have been forbidden from entering Beijing since 2014.

3.2 Impact of local emissions on air quality

The average diurnal profiles in [figFig. 5](#) highlight the relationship between emissions, [mixing-mixed](#) layer height and concentrations. Whilst emissions and concentrations seem to be closely linked when averaged over the whole campaigns, there are periods where local emissions do not drive concentrations. During the winter months Beijing experiences a frequent cycling between “polluted” and “clean” days and this phenomenon has been termed “sawtooth cycles”. During winter pollutants build up during near stagnant periods with SE wind flow being trapped by the mountain range in the NW. These are then advected out of the city when wind speed increases and the direction switches to the NW resulting in sharp reductions in atmospheric concentrations (Jia et al., 2008; Li et al., 2017). This distinctive meteorological phenomenon occurs in Beijing as a result of the East Asian Winter Monsoon, itself driven by temperature differences between the Pacific Ocean and Asian continent (Chen et al., 1992). This cycling was observed during the winter field campaign and can be seen in NO_x and CO concentrations highlighted in [figFig. 4](#). During the period 21 November 2016 – 23 November 2016 average daytime concentrations of $0.020\text{mg}\cdot\text{m}^{-3}$ and $0.35\text{mg}\cdot\text{m}^{-3}$ for NO_x and CO respectively were observed. On the following three days, 24 November 2016 – 27 November 2016, higher concentrations of $0.13\text{mg}\cdot\text{m}^{-3}$ of NO_x and $1.7\text{mg}\cdot\text{m}^{-3}$ of CO were measured, a more than five-fold increase in average daytime concentrations compared with the “clean” period. Corresponding [increase-increases](#) and decreases in pollutant flux [was-were](#) not clearly observed however ([figFig. 4](#)). Figure 6 shows the distribution of the NO_x and CO fluxes and concentrations over the “clean” and “polluted” days. Despite the higher concentrations during the polluted period the measured flux is slightly lower. During the polluted period more deposition flux occurred; 13 % of NO_x fluxes and 23 % of CO fluxes (associated with u_* values over $0.175\text{m}\cdot\text{s}^{-1}$) were negative whereas no deposition fluxes were measured during the clean period.

Figure 7 shows two flux footprints; one averaged for the clean period and one for the polluted period. Satellite images and Open Street Map data ([openstreetmap.org](#)) shows that these footprints cover very similar land use areas; predominantly residential with busy roads so it is expected that the emissions would be similar for these areas, consistent with the variability in the measured flux. This indicates concentrations were more affected by meteorology, driving the accumulation at the city scale, or transport from regions outside Beijing than local emissions. There was not a significant contrast between mean [mixing-mixed](#) layer heights between the two periods. A mean height of 464 m (including nighttime and daytime) with a daytime maxima of 811 m for the clean period was measured. For the polluted period the mean [mixing-mixed](#) layer height was 434 m with a daytime maxima of 822 m. Wind speeds were much lower during the polluted period with a mean wind speed of $1.9\text{m}\cdot\text{s}^{-1}$

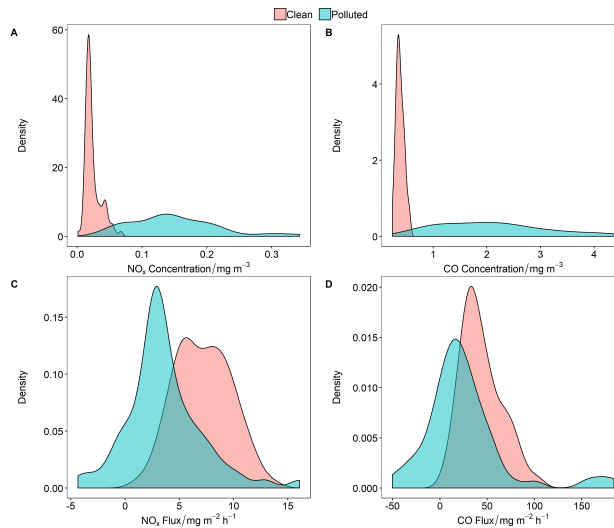


Figure 6. The density distribution of NO_x and CO concentrations and fluxes during the “clean” period (21 November 2016 – 23 November 2016) and “polluted” period (24 November 2016 – 27 November 2016). Only fluxes for which u_* values are over 0.175 m s^{-1} and which meet the 60 % stationarity criteria are presented to allow a valid comparison.

compared to 6.0 m s^{-1} for the clean period. These more stagnant conditions cause emissions to build up before being advected out of the city when wind speeds increase once again. Additionally, the higher wind speeds experienced during the “clean” period mean the city is influenced by air masses from further away. To the north-west, the dominant wind direction for the “clean” period, there is less industrial activity compared to the south of the measurement site towards the centre of Beijing, so these air masses are also likely to be less polluted.

3.3 Dependence on wind direction

Examining the relationship between diurnal flux and wind direction can give further information about emission sources. Figure 8 shows the average diurnal emission NO_x and CO flux plotted as a function of wind direction for both the winter and summer campaigns. Hour of day is represented by the radial scale between the inner and outer rings and starts at 00:00 in the inner side of the ring to 23:00 on the outer side of the ring.

For the winter campaign there appears to have been an enhancement in flux when there is a northerly wind direction. For NO_x the emission was largest throughout the afternoon hours but for CO peaks are more distinct, with an enhancement at midday and again between 16:00 – 20:00. Within the flux footprint, to the north of the site are residential areas, Beitucheng West Road (a busy traffic route) as well as some university buildings and a hospital. Further north (approximately 1 km from the tower) is the fourth ring road. The largest NO_x fluxes were observed between 16:00 – 20:00 when the wind direction was westerly. Within this wind sector lies Beitapingzhuang Road, about 0.65 km from the tower and Xueyuan Road which links the third and fourth ring roads slightly further to the west and just under 2 km away from the tower.

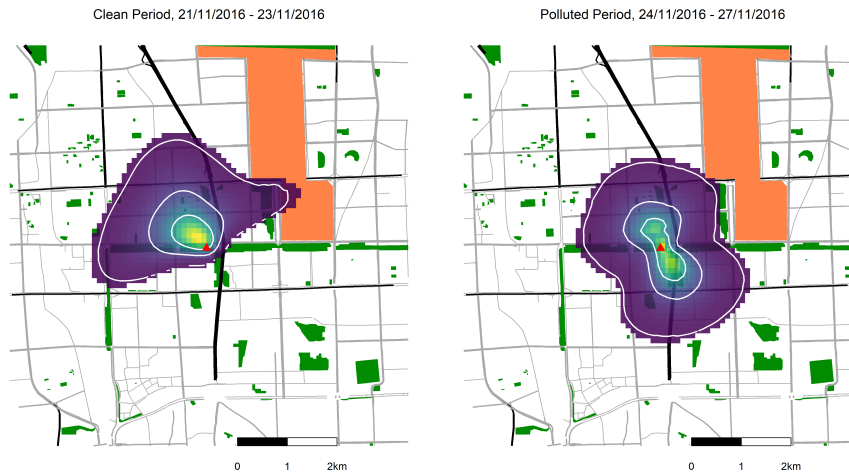


Figure 7. The left-hand plot shows the average footprint [Average footprints](#) for the “clean” period, 21 November 2016 – 23 November 2016 (left) and the right-hand plot the average footprint for the “polluted” period, 24 November 2016 – 27 November 2016 (right). Map was built using data from © OpenStreetMap contributors 2019. Distributed under a Creative Commons BY-SA License.

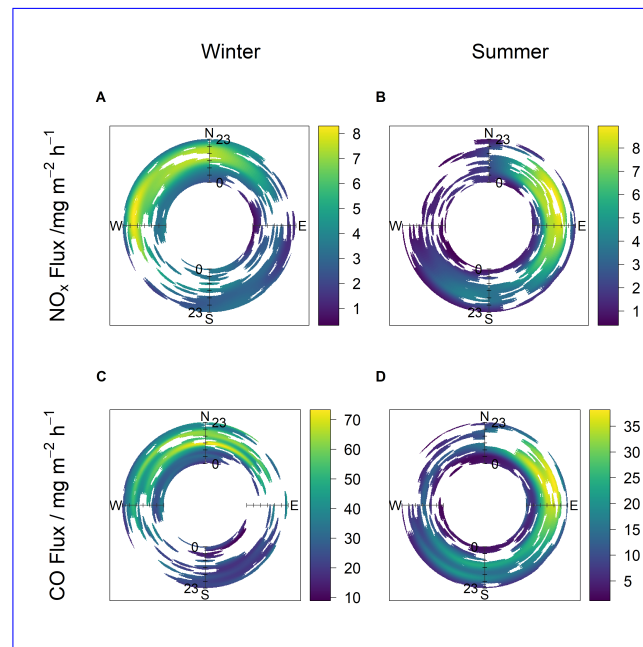


Figure 8. Polar annulus plots for NO_x and CO fluxes for both campaigns, showing the relationship between mean diurnal flux and wind direction. 0 – 23 refers to hour of day and the colour scale shows flux in mg m⁻² h⁻¹.

Table 2. Summary table for VOC concentrations and fluxes measured by PTR-MS/PTR-ToF-MS. Data presented is for fluxes which are within 60 % stationarity criteria for all u_* values.

	Winter				Summer			
Conc (mg m ⁻³)	Benzene	Toluene	C2-Benzene	C3-Benzene	Benzene	Toluene	C2-Benzene	C3-Benzene
Mean	0.00703	0.00808	0.00975	0.00258	0.00186	0.00257	0.00390	0.00127
Median	0.00532	0.00620	0.00688	0.00198	0.00173	0.00227	0.00336	0.00113
Percentiles								
5th	0.000910	0.00100	0.00121	0.000431	0.000860	0.00113	0.00166	0.000572
95th	0.0190	0.0225	0.0299	0.00658	0.00346	0.00502	0.00794	0.00245
Standard Deviation	0.00618	0.00707	0.00969	0.00198	0.000864	0.00227	0.00237	0.000677
Flux (mg m⁻² h⁻¹)								
Mean	0.0121	0.0640	0.0730	0.00357	0.101	0.307	0.236	0.148
Median	0.0197	0.00861	0.00656	0.00354	0.0858	0.197	0.131	0.0995
Percentiles								
5th	-0.296	-0.209	-0.270	-0.0662	0.0180	0.137	-0.0166	0.0207
95th	0.195	0.427	0.692	0.0737	0.237	0.872	0.941	0.479
Standard Deviation	0.184	0.249	0.286	0.0455	0.0736	0.363	0.374	0.151

During the summer campaign, there was an enhancement in the daytime flux of CO and NO_x with an easterly wind, indicating of an emission source to the east of the site; probably the Jingzang Highway just 0.35 km east of the site as shown in figFig. 1. There are also some daytime enhancements in NO_x and CO emissions from the south of the measurement site towards central Beijing. For CO, enhancements to the south show two quite distinct enhancement periods in the morning and evening, 5 suggesting these emissions are from vehicles. It is unlikely that there were any significant seasonal change in traffic density on roads surrounding the measurement site. The change from a westerly influence observed during the winter to an easterly influence in summer is due to changes in the dominant wind direction. Beijing's wind patterns are quite different during the winter and the summer. There is a noticeable absence of easterly winds in the winter and the mean flux footprints (figFig. 3) highlights-highlight the difference in regions contributing to the observed flux.

10 3.4 Comparison with VOC Flux

Aromatic hydrocarbons, including benzene, C₂-benzene, C₃-benzene and toluene are components of gasoline fuel and are typically emitted from combustion and evaporation of fuels and solvents in urban environments (Caplain et al., 2006; Langford et al., 2009). Table 2 summarises the fluxes and concentrations measured during the APHH-Beijing measurement campaigns. Concentrations were significantly greater during the winter season while emissions were higher during the summer for all four 15 hydrocarbon species. During the summer, toluene fluxes were the largest (0.31mg m⁻²-mg m⁻² h⁻¹), followed by C₂-benzene (0.24mg m⁻²-mg m⁻² h⁻¹) then C₃-benzene (0.15mg m⁻²-mg m⁻² h⁻¹) and the flux of benzene being the smallest (0.10mg m⁻²

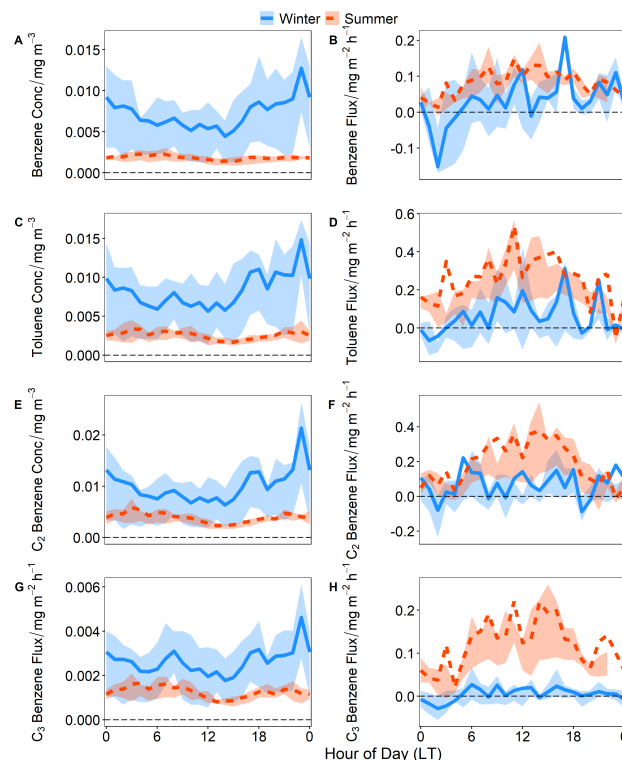


Figure 9. ~~Seasonal variation in diurnal profile~~ Diurnal profiles for A) benzene concentration, B) benzene flux, C) toluene concentration, D) toluene flux, E) C₂-benzene concentration, F) C₂-benzene flux, G) C₃-benzene concentration and H) C₃-benzene flux measured by PTR-MS/PTR-ToF-MS. Blue, solid lines are for measurements taken during the winter campaign and the orange, dashed lines are measurements taken during the summer campaign. The shaded areas represent the 25th and 75th percentiles to give an idea of the spread of the data. Only stationary data has been used but no u_* filtering has been applied when doing the diurnal averaging.

$\text{mg m}^{-2} \text{h}^{-1}$). Diurnal variation of VOCs for winter and summer is shown in ~~fig~~ Fig. 9. The uncertainty in the diurnal averages makes drawing conclusions about variations between daytime and nighttime difficult, although there are some indications that summertime trends at least may mimic those of CO and NO_x. During summer, fluxes of all four species followed a very similar diurnal trend with generally higher emissions in the daytime compared to the nighttime. A smaller early morning peak was observed at 08:00, slightly later than the morning peak in NO_x emissions which reached their maximum at 07:00. Emissions increased again in the afternoon for toluene, C₂-benzene and C₃-benzene peaking between 15:00 – 16:00. Benzene remained fairly constant throughout the afternoon with a mean emission of $0.076 \text{mg m}^{-2} \text{h}^{-1}$. The peak during the night corresponds to a one-off event measured on the 29/05/2017 at 03:30. During the winter, C₂-benzene fluxes were the largest ($0.073 \text{mg m}^{-2} \text{h}^{-1}$), followed by the toluene flux ($0.064 \text{mg m}^{-2} \text{h}^{-1}$), then benzene ($0.012 \text{mg m}^{-2} \text{h}^{-1}$) with the flux of C₃-benzene flux ($0.0036 \text{mg m}^{-2} \text{h}^{-1}$) being the smallest. There was no clear difference between nighttime and daytime emissions for all species.

Table 3. Summary of mean VOC fluxes measured in various urban or semi-urban locations.

VOC Species	Mean Flux /mg m ⁻² h ⁻¹	Location and Year	Reference
Benzene	0.0121	Beijing (, November – December 2016)	<i>This study</i>
	0.101	Beijing (, May – June 2017)	<i>This study</i>
	4.7*	Mexico City, March – April 2006	Karl et al. (2009)
	0.396	Mexico City, March 2006	Velasco et al. (2009)
	0.12	Manchester, June 2006	Langford et al. (2009)
	0.15	London, October 2006	Langford et al. (2010)
	<u>0.17</u>	<u>Houston, May – July 2008</u>	<u>Park et al. (2010)</u>
	0.09	London, August – December 2012	Valach et al. (2015)
	0.02	Helsinki (urban background), January 2013 – September 2014	Rantala et al. (2016)
	0.07*	Central London, July 2013	Vaughan et al. (2017)
	<u>0.02</u>	<u>Innsbruck, July – October 2015</u>	<u>Karl et al. (2018)</u>
Toluene	0.0.0640	Beijing (, November – December 2016)	<i>This study</i>
	0.307	Beijing (May – June 2017)	<i>This study</i>
	0.83	Mexico City, April 2003	Velasco et al. (2005)
	14.1*	Mexico City, March – April 2006	Karl et al. (2009)
	3.1	Mexico City, March 2006	Velasco et al. (2009)
	0.28	Manchester, June 2006	Langford et al. (2009)
	<u>0.58</u>	<u>Houston, May – July 2008</u>	<u>Park et al. (2010)</u>
	0.41	London, August – December 2012	Valach et al. (2015)
	0.051	Helsinki (urban background), January 2013 – September 2014	Rantala et al. (2016)
	0.24*	Central London, July 2013	Vaughan et al. (2017)
	<u>0.08</u>	<u>Innsbruck, July – October 2015</u>	<u>Karl et al. (2018)</u>
C2-Benzene	0.0730	Beijing(, November – December 2016)	<i>This study</i>
	0.236	Beijing(, May – June 2017)	<i>This study</i>
	0.468	Mexico City, April 2003	Velasco et al. (2005)
	1.3	Mexico City, March 2006	Velasco et al. (2009)
	0.32	Manchester, June 2006	Langford et al. (2009)
	0.28	London, October 2006	Langford et al. (2010)
	0.059	Helsinki (urban background), January 2013 – September 2014	Rantala et al. (2016)
	0.32*	Central London, July 2013	Vaughan et al. (2017)

*Measured from an aircraft.

Table 3 summarises previous urban flux measurements to allow the VOC fluxes from Beijing to be put into context. The benzene fluxes measured in Beijing during summer fall into the range of those reported in ~~table~~ Table 3 and are most similar to values reported for large cities in the UK. Toluene fluxes and C₂-benzene fluxes measured during the summer in Beijing are also similar to the mean fluxes measured in UK cities where vehicular emissions were found to dominate aromatic fluxes.

5 However, it should be noted that previous measurements over London were all made with a quadrupole PTR-MS instrument, which, unlike the time-of-flight instrument used in the present study, is restricted to a unit mass resolution. This means that the benzene, toluene and C₂-benzene signals may have included contributions from other compounds and therefore is likely to be an overestimate of the true C₂-benzene emission. The VOC flux values reported for Mexico City are much greater than those measured in Beijing for both seasons. Karl et al. (2009) reported an influence from evaporative emissions from the northern

10 industrial district but there is no industrial emission source within the flux footprint for the Beijing measurements. This, along with a more modern vehicle fleet subject to stricter emissions regulation in Beijing may explain the larger discrepancy between these two cities. Fluxes measured in Helsinki are lower than emissions measured in the summer but comparable to those measured during the winter.

Emissions of all four species were higher in summer than in winter, although the statistical significance of all but C₃-

15 benzene is somewhat uncertain. This is the opposite to the trend observed for NO_x and CO emissions, most likely driven by higher evaporation rates due to higher temperatures. The mean daytime temperature was 281 K during the winter campaign and 305 K during the summer campaign. Comparing VOC fluxes to NO_x and CO fluxes in the summer, emissions of C₂-benzene and C₃-benzene started to increase in the early hours of the morning (05:00) as observed for NO_x and CO, indicating a rapid release of emissions from a new source, such as traffic emissions. This is true for toluene and benzene, although the relative

20 difference between night and day emissions is less pronounced. All four hydrocarbon species ~~peak~~ showed an enhancement during the mid-morning during the summer, like CO, probably due to an additional contribution from residential and cooking emissions from local restaurants. There is possibly a winter contribution from evening rush hour traffic to the benzene and toluene emissions that mirrors that observed in the CO and NO_x emissions at 17:00, though this is not clearly observed during the summer campaign. During the summer, the ~~emission for~~ emissions of all four species are elevated in the afternoon (between

25 13:00 – 18:00) when temperatures are highest. These emissions are likely enhanced by evaporation which masks the evening rush hour traffic contribution. There is a strong correlation between total VOC flux and heat flux in summer ($r = 0.83$) compared to the winter ($r = 0.35$).

The ratio of benzene to toluene (B/T) is often used to gauge the photochemical age of an air mass as the two species have different atmospheric lifetimes due to their different ~~reactivities~~ reactivity with the OH radical. Heeb et al. (2000) reported B/T

30 concentration ratios between 0.41 – 0.83 for primary exhaust emissions. As an air mass ages, the ratio increases as toluene is more reactive than benzene. For Beijing, the median B/T concentration ratio in the winter was 0.89 and 0.73 for the summer at the upper end of the expected range for primary exhaust emissions. Barletta et al. (2005) reported a roadside B/T value of 0.6 for Beijing, however vehicle fleet and fuel types are rapidly changing in response to legislation so this measurement may not be representative for the measurement period of this work. The difference in B/T concentration ratios does however

35 indicate that VOC sources are changing between winter and summer as the change in ratio cannot be explained by ~~temperature~~

~~differences expected changes in atmospheric oxidation rates caused by seasonal differences in temperature~~. Langford et al. (2009) points out that temperature can impact B/T ratios as reactivity rates ~~increases increase~~ with warmer temperatures but if temperature was driving the seasonal difference it would be expected that ~~the~~ B/T ratio measured during summer is higher than during winter. It is likely that additional sources such as domestic burning and cooking are present in winter; Barletta et al. (2005) reports that higher B/T concentration ratios are associated with natural gas and biomass combustion, which supports the hypothesis that these type of emission sources could be leading to an increased B/T concentration ratio in the winter. The B/T flux ratio should reflect better the ratio of the two pollutants in emissions sources as flux ratios are confined to the area of the flux footprint rather than being influenced by a wider area (Karl et al., 2009). The median B/T flux ratios were 0.72 for the winter campaign and 0.31 for the summer campaign, further suggesting a change in emission source between the two seasons. The B/T flux ratio for summer is lower than expected for primary exhaust emissions though similar values have been reported for vehicles without catalytic converters (Heeb et al., 2000) and given higher temperatures, emissions from other sources such as solvent evaporation, may affect this ratio. Indeed, Karl et al. (2009) showed that fuel evaporative losses typically have a higher toluene fraction, leading to lower B/T ratios. The strong VOC-heat flux correlation and the low B/T ratio observed during the summer campaign suggests fuel evaporative loss is a source of aromatic VOC emissions in Beijing.

15 3.5 Comparison with an Emissions Inventory

The measured NO_x and CO fluxes were compared to the high-resolution (3 km \times 3 km) MEIC v1.3 inventory ~~and the mean diurnal profiles are presented in fig. 10 with a base year of 2013~~. The comparison of VOC emissions with an emissions inventory is beyond the scope of this work. ~~Comparison of measured diurnal trend and diurnal trend predicted by the MEIC inventory for NO_x and CO. Panels A and B show NO_x and CO emissions for the winter campaign and panels C and D NO_x and CO emissions from the summer campaign. Four sections of the inventory are presented alongside the measured emission as a black dashed line. For both winter and summer, the inventory grossly overestimates emissions of~~ A direct comparison of the diurnal variation in measured emissions and that in the inventory indicates that NO_x and CO emissions are grossly overestimated throughout the day for both campaigns. Total NO_x emissions are overestimated by a factor of 3.8 – 17 (mean overestimation of 9.9 throughout the day) in the winter and 4.2 – 25 (mean = 11) in the summer. For CO, winter emissions were between 1.6 – 9.7 (mean = 4.8) times larger in the inventory than those measured and summer emissions between 5.2 – 21 (mean = 10) times larger.

Part of the discrepancy between the inventory and measured emissions may be due to the comparison of observations (made in 2016/2017) with an older inventory (base year 2013). China's NO_x emissions have rapidly changed in the past three decades. Liu et al. (2016) report that between 2005 and 2011 NO_2 emissions increased by 53 % for the whole of China, attributed for the most part to increasing fuel consumption with coal the dominant fuel type. An estimated three-quarters of all electricity in China was generated by coal in 2016 (International Energy Agency, 2016). After 2012 however, a combination of the installation of power plant de-nitration devices and vehicle emissions controls has led to a 32 % decrease in NO_2 emissions (Liu et al., 2016; Krotkov et al., 2016; Miyazaki et al., 2017). In Beijing, NO_x emissions are decreasing thanks to numerous air pollution control measures implemented since 2000; polluting industries and power plants have been relocated outside of

the city, stricter emissions standards for industrial and domestic boilers have been introduced and the fuel type shifted from coal to gas (Wang et al., 2010). Since the introduction of the “Clean Air Action Plan” in Beijing in 2013, 900,000 households in Beijing have converted from using coal to cleaner technologies like gas or electricity. The burning of biomass, such as wood and crops, was completely forbidden by the end of 2016 (Cheng et al., 2019). The impact of the emissions controls has been predicted to reduce emissions of NO_x and VOCs by 43 % and 42 % respectively between 2013 – 2017 in Beijing (Cheng et al., 2019). Most significant for NO_x emissions however is the stringent vehicle control measures introduced within the last decade, accounting for 47 % of the total reduction in emissions for the city.

CO emissions have also been declining in Beijing over the past two decades by an average rate of 1.14 % year⁻¹ (Wang et al., 2018). Zheng et al. (2018) highlight a reduction in inefficient domestic stoves and improvements in emissions standards for vehicles as being dominant forces for the observed reduction in CO emissions. For VOCs, vehicle emission controls were another significant contributor to the reduction with 16.1 % of the reduction attributed to new controls. Improvements in management of solvent use (e.g. use of high-solid and waterborne paints instead of solvent based ones) dominated the reduction in VOC emissions contributing 49.3 % to the total reduction in Beijing. Emissions between 2013 – 2016 were predicted to reduce by 30 % for NO_x and 35 % for VOCs (Cheng et al., 2019; Biggart et al., 2020).

These estimated changes were applied to the inventory leading to reductions in emissions of 30 % in the winter and 43 % for the summer for both species. No emissions reductions were presented for CO alone but given that its expected sources are similar to NO_x the same reduction factor was applied to the CO inventory emissions. The mean diurnal profiles for the lowered inventory estimates are presented in Fig. 10, with measured emissions shown by the black dashed line. With the expected reduction considered, NO_x is still overestimated by a factor of 2.7 – 12 (mean = 7.0) in the winter and 2.4 – 14 (mean = 6.8) times in the summer. Similarly, CO emissions are still overestimated for both seasons with inventory CO emissions 1.1 – 6.8 (mean = 3.4) times larger than the measured CO emission for the winter campaign. For summer, the inventory overestimated CO emissions by a factor of 2.9 – 12 (mean = 5.6) times. The closest agreements between inventory and measurements were during the nighttime in all cases. Applying these reductions does obviously improve the inventory comparison, compared with the original, however large overestimations remain.

Examination of the flux footprint suggests that the majority of measured emissions are coming from transportation and residential sources. The inventory supports this for CO, suggesting that transportation is the largest contributing sector, followed by the residential sector. However, for NO_x the inventory also suggests that there is a large industrial source, contributing up to 60 % to the total emissions for the winter campaign and 52 % for the summer campaign. No obvious industrial sources could be identified within the flux footprint for this study. Zheng et al. (2017) observed a decoupling between real world emissions and the spatial proxies used to develop [and downscale](#) inventories as polluting industries are moved out of urban centres. The methods used to allocate emissions in the MEIC inventory appear to result in emissions being overestimated in the urban area of Beijing; spatial proxies such as population density and Gross Domestic Product (GDP) are used to scale down national emissions statistics. This method tends to overestimate emissions in urban centres and underestimate emissions in rural areas and so even if this comparison only considered the residential and transport sectors, NO_x and CO emissions would still be **significantly** overestimated by the inventory. Just considering these two sectors, NO_x emissions are overestimated by a factor ~~2.4~~~~1.6~~ – ~~7.3~~~~5.1~~ (mean = ~~4.7~~~~3.3~~) for winter and ~~3.4~~~~1.9~~ – ~~15~~~~8.5~~

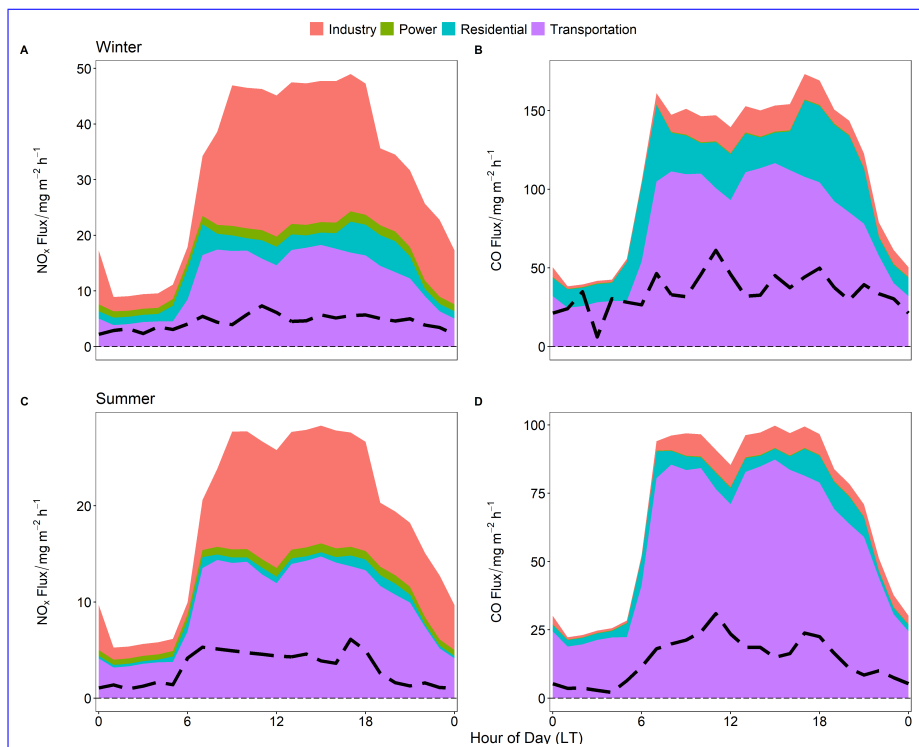


Figure 10. Measured diurnal trend (dashed black line) and predicted diurnal trend using the MEIC inventory (filled areas by sector) for NO_x and CO emissions. MEIC inventory data has been reduced by 30 % for comparison with the winter 2016 campaign and by 43 % for comparison with the summer 2017 campaigns to take account of expected emissions reductions indicated in Cheng et al. (2019). Panels A and B show emissions for the winter campaign and panels C and D show emissions from the summer campaign.

(mean = 6.53.7) for summer. CO emissions are overestimated by 1.5-1.1 – 9.2-6.5 (mean = 4.43.1) in winter and 4.7-2.7 – 20.12 (mean = 9.25.2) in summer. The sensitivity of the inventory to location was tested by shifting the inventory grid 3 km in each direction (north, east, south and west) and it was found that this had little impact on the comparison with the inventory still overestimating emissions for all directions.

- 5 The inventory did capture some of the general diurnal variation in emissions. Figure 11 shows the normalised diurnal variation for the transportation and residential sectors, calculated relative to one another assuming these sectors are the only emission sectors. The diurnal variation in measured emissions normalised by the daily average is overlaid. For NO_x and CO emissions in the winter (Fig. 11, panels A and B) the sum of the residential and transportation emissions captures the time of the morning rush hour peak at 07:00 and the evening enhancement in emissions in the mid-afternoon to evening due to a combination of increased residential and traffic activity. Residential emissions are predicted in the inventory to increase between 11:00 – 12:00 which was observed in the measurements, though to a greater extent than the inventory suggests.
- 10

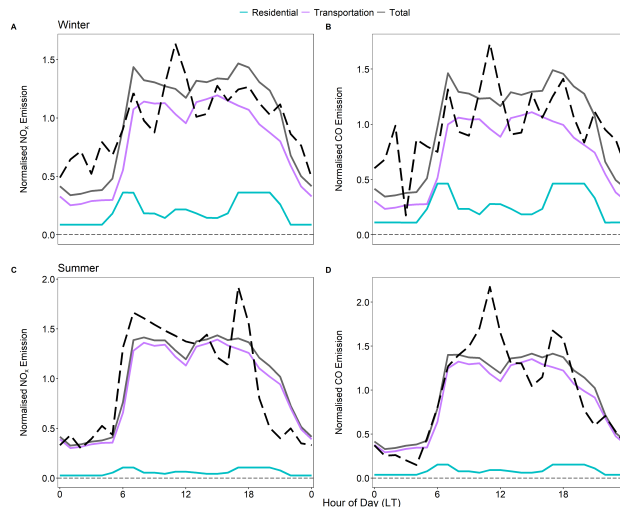


Figure 11. Comparison of normalised diurnal variation in NO_x and CO emission predicted by the MEIC inventory and measured flux. The normalised emission has been calculated for the inventory by dividing hourly sector emission by the mean daily sector emission. Given there are no clear industrial or power generation emission sources within the flux footprint, only the residential (blue solid line) and transportation (purple solid line) sectors have been presented. The normalised diurnal variation for these sectors have been multiplied by the normalised diurnal variation for the sum of the residential and transportation sectors (grey solid line) to reflect the relative contributions of the two sectors. Normalised diurnal variation in the measured emission has been calculated by dividing mean hourly emission by mean daily emission (black dashed line). Panels A and B show data for NO_x and CO from the winter campaign and panels C and D for the summer.

Looking at the summer data for NO_x (Fig. 11, panel C), the increase in emissions after 05:00 when traffic density increased was well captured for NO_x though the [measurement measurements](#) suggested a slightly quicker increase in emission than suggested by the inventory. The minimum daytime emission predicted by the inventory occurred at 12:00 where there was a dip in emissions from transportation though this was not reflected in the measurements where there was an almost constant decrease in NO_x emissions until the evening rush hour peak at 17:00. The evening rush hour peak for NO_x in summer was much more distinct than the inventory suggests and NO_x emissions decrease rapidly after 18:00, earlier than the inventory predicts. NO_x emissions from residential sources in the inventory showed a small enhancement around midday which was not clearly observed in the [measurement measurements](#), suggesting traffic related emissions dominate here. For CO in summer (Fig. 11 panel D), the increase in measured emissions after 05:00 matches the rate of increase predicted by the inventory very well. After 07:00 the inventory predicted CO emissions would not increase further which was not reflected in the measured emissions. Emissions from the residential sector are predicted to increase between 11:00 – 12:00 reflecting emissions from cooking activities. Within the flux footprint there were several restaurants including barbecue restaurants where food was cooked over open coals. This is not likely to be included in the inventory but would explain the increase in measured CO emissions before lunchtime as food is prepared. As with NO_x emissions, the evening rush hour peak in measured CO emissions was narrower and began to decrease earlier than suggested by the inventory.

The inventory suggests that total emissions are higher in winter than in summer; NO_x emissions from the residential and transportation sectors are between ~~1.1–1.3~~–~~1.4–1.7~~ times larger and for CO emissions from these two sectors are between ~~1.2–1.5~~–~~1.6–2.0~~ times larger. The inventory performs relatively well capturing the measured seasonal difference ~~in NO_x (for emissions of both species. The seasonal difference in NO_x emissions are slightly overestimated (measured~~ emissions were on average 1.2 times greater in winter compared to summer) ~~but not for CO (and the inventory underestimates the seasonal difference in CO emissions (measured~~ emissions were on average 2.3 times higher in winter than summer). ~~Inventory NO_x emissions for transportation are almost identical for the two seasons whilst residential emissions vary by a factor of four. The inventory attributes seasonal differences in CO emissions chiefly to the residential sector, estimating approximately a 4 fold increase in residential emissions in winter compared to summer. CO emissions from the transportation sector are between 1.05–1.09 times higher in winter than summer suggesting any effects of vehicle cold starts and reduced engine combustion efficiencies are not represented in the inventory ; something that was considered the main source of seasonal variation in CO fluxes in London (Helfter et al., 2016). Aside from the error introduced through the use of the spatial proxies for scaling, discrepancies between inventory and measurements are likely to be due to the comparison of observations (2016/2017) with an older inventory (2013). China’s NO_x emissions have rapidly changed in the past three decades. Liu et al. (2016) report that between 2005 to 2011 NO₂ emissions increased by 53 % for the whole of China, attributed for the most part to increasing fuel consumption with coal the dominant fuel type. An estimated three-quarters of all electricity in China was generated by coal in 2016 (International Energy Agency, 2016). After 2012 however, a combination of the installation of power plant de-nitration devices and vehicle emissions controls has led to a 32 % decrease in NO₂ emissions (Liu et al., 2016; Krotkov et al., 2016; Miyazaki et al., 2017). In Beijing, NO_x emissions are decreasing thanks to numerous air pollution control measures implemented since 2000; polluting industries and power plants have been relocated outside of the city, stricter emissions standards for industrial and domestic boilers have been introduced and the fuel type shifted from coal to gas (Wang et al., 2010). Since the introduction of the “Clean Air Action Plan” in Beijing in 2013 For both NO_x and CO the inventory suggests that seasonal variation is driven by increased residential sector emissions, 900,000 households in Beijing have converted from using coal to cleaner technologies like gas or electricity. The burning of biomass, such as wood and crops, was completely forbidden by the end of 2016 (Cheng et al., 2019). The impact of the emissions controls has been predicted to reduce emissions of NO_x and VOCs by 43 % and 42 % respectively between 2013–2017 in Beijing (Cheng et al., 2019). Most significant for NO_x emissions however is the stringent vehicle control measures introduced within the last decade, accounting for 47 % of the total reduction in emissions for the city. CO emissions have also been declining in Beijing over the past two decades by an average rate of 1.14 % year⁻¹ (Wang et al., 2018) -Zheng et al. (2018) highlight a reduction in inefficient domestic stoves and improvements in emissions standards for vehicles as being dominant forces for the observed reduction in CO emissions. For VOCs, vehicle emission controls were another significant contributor to the reduction with 16.1 % of the reduction attributed to new controls. Improvements in management of solvent use (e.g. use of high solid and waterborne paints instead of solvent based ones) dominated the reduction in VOC emissions contributing 49.3 % to the total reduction in Beijing. Emissions between 2013–2016 were predicted to reduce by 30 % for NO_x and 35 % for VOCs (Cheng et al., 2019; ?). Taking these reductions into account and lowering the inventory emissions by 30 % in the winter and 43 % for the summer NO_x is still overestimated by a factor of 1.6–7.2 in the winter and~~

1.6—9.0 times in the summer. No emissions reductions were presented for CO alone but given that its expected sources are similar to NO_x the same reduction factor was applied to the CO inventory emissions. With this reduction taken into account CO emissions predicted by the inventory were at times lower than those measured during the night, with the inventory CO emissions being 0.84—5.0 times the measured CO emission. For summer, the inventory overestimated CO emissions by a factor of 2.2—9.0 times. The closest agreements between inventory and measurements were during the nighttime in all cases. Applying these reductions does obviously improve the inventory comparison however given the large overestimations it is likely that the uncertainty caused by use of spatial proxies when developing the inventory is the main one. which are predicted to be 5 times higher in winter than summer.

4 Summary

NO_x, CO and aromatic VOC emissions have been quantified for the first time during two contrasting seasons for an area of central Beijing. The magnitude of NO_x emissions were found to be similar during the winter and summer periods whilst the fluxes of CO showed a greater seasonal dependence with winter emissions being over 2 times greater than CO emissions measured during summer. The dominant source for NO_x and CO emissions is traffic with influence from residential emissions. The diurnal variation in aromatic VOCs fluxes also suggested traffic and residential sources, though evaporative effects due to higher summer temperatures meant emissions were greater in the summer than the winter. The NO_x and CO fluxes presented in this work provide good evidence that proxy-based inventories can overestimate emissions for urban centres as suggested by Zheng et al. (2017). When developing inventories at an urban scale future work should look carefully at up-to-date proxies or at deriving emissions by bottom-up approaches in order to correctly predict the magnitude of emissions. When comparing the diurnal variation in inventory and measurement the inventory performed relatively well capturing morning and evening rush hour peaks. The inventory also attributed traffic and residential emissions as the major source of NO_x and CO emissions which was supported by analysis in this work. This set of pollutant flux measurements can provide a useful basis for developing these high resolution urban inventories which are at an appropriate scale to assess public health impacts of pollution.

Appendix A

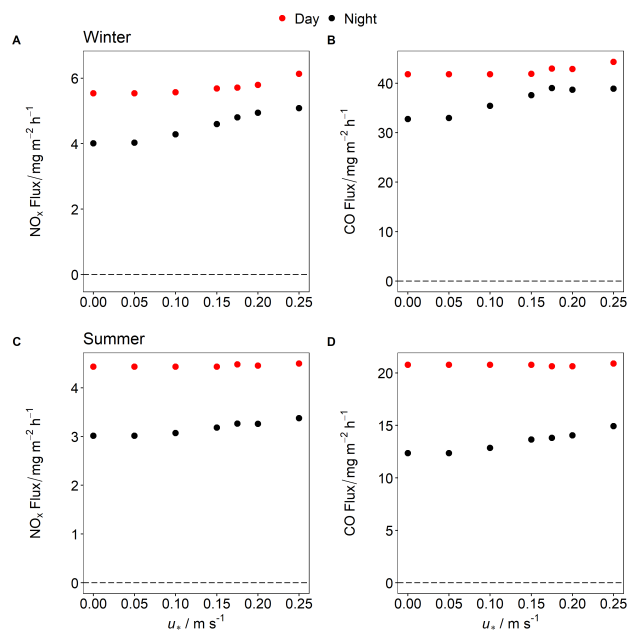


Figure A1. Mean NO_x and CO fluxes as a function of different u_* thresholds.

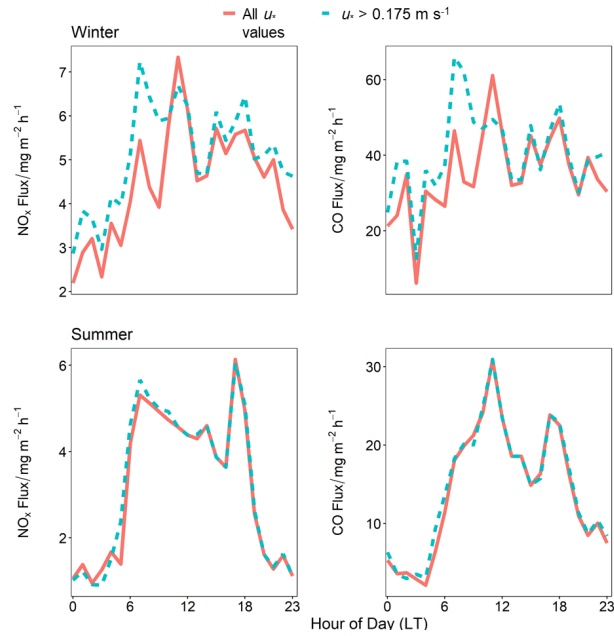


Figure A2. Comparison between diurnal variation in NO_x and CO fluxes for all u_* values and for u_* values over 0.175.



Figure A3. MEIC inventory emission grids for NO_x and CO for November. Map was built using data from © OpenStreetMap contributors 2019. Distributed under a Creative Commons BY-SA License.

- Author contributions.* FAS made NO_x and CO concentration measurements, calculated their flux and analysed the data presented. FAS prepared the manuscript with contributions from co-authors. EN and BL measured wind vector data used in this study, set up tower instrumentation, provided extensive advice on flux calculations and provided detailed comments on the manuscript. OW assisted with interpretation of the inventory emissions data and gave ideas for analysis. WSD provided support calculating NO_x and CO fluxes and reviewed the manuscript.
- 5 WJFA and MS made VOC concentration measurements during the field campaigns and assisted with interpretation of the VOC fluxes. MH processed the raw emissions data into gridded format for comparison with the measured fluxes. SBG and SK provided boundary layer height data. ND and SM provided support on using eddy4R software for data processing and reviewed the manuscript. QZ and RW provided high resolution emissions data. XW and YZ prepared the PTR-ToF-MS instrument and calibration system. PF maintained the tower and site necessary for this work. CNH, JFH and JL reviewed the manuscript.
- 10 *Competing interests.* The authors declare that they have no conflict of interest.

Acknowledgements. This work was supported by the UK Natural Environment Research Council and the Newton fund through the AIR-POLL project of the Air Pollution and Human Health in a Chinese Megacity (APHH-Beijing) programme (grant references NE/N006917/1, NE/N006992/1 and ~~NE/N006976/1~~ [and NE/N00700X/1](#)). The authors would like to thank Rachel Dunmore and Neil Mullinger for their hard work during the field campaigns. Thanks also go to Shona Wilde and Stuart Grange for their assistance creating plots for this work.

References

- Acton, W. J. F., Huang, Z., Davison, B., Drysdale, W. S., Fu, P., Hollaway, M., Langford, B., Lee, J., Liu, Y., Metzger, S., Mullinger, N., Nemitz, E., Reeves, C. E., Squires, F. A., Vaughan, A. R., Wang, X., Wang, Z., Wild, O., Zhang, Q., Zhang, Y., and Hewitt, C. N.: Surface-atmosphere fluxes of volatile organic compounds in Beijing, *Atmos. Chem. Phys. Discuss.*, 2020, 1–36, <https://doi.org/10.5194/acp-2020-343>, 2020.
- Andreae, M. O. and Schimel, D. S.: Exchange of trace gases between terrestrial ecosystems and the atmosphere, John Wiley and Sons Inc., New York, USA, <https://doi.org/10.1007/BF00024600>, 1990.
- Aubinet, M.: Eddy covariance CO₂ flux measurements in nocturnal conditions: An analysis of the problem, *Ecol. Appl.*, 18, 1368–1378, <https://doi.org/10.1890/06-1336.1>, 2008.
- 10 Barletta, B., Meinardi, S., Rowland, F. S., Chan, C.-Y., Wang, X., Zou, S., Chan, L. Y., and Blake, D. R.: Volatile organic compounds in 43 Chinese cities, *Atmos. Environ.*, 39, 5979–5990, <https://doi.org/10.1016/j.atmosenv.2005.06.029>, 2005.
- Biggart, M., Stocker, J., Doherty, R. M., Wild, O., Hollaway, M., Carruthers, D., Li, J., Zhang, Q., Wu, R., Kotthaus, S., et al.: Street-scale air quality modelling for Beijing during a winter 2016 measurement campaign., *Atmos. Chem. Phys.*, 20, <https://doi.org/10.5194/acp-20-2755-2020>, 2020.
- 15 Borbon, A., Gilman, J. B., Kuster, W. C., Grand, N., Chevaillier, S., Colomb, A., Dolgorouky, C., Gros, V., Lopez, M., Sarda-Esteve, R., Holloway, J., Stutz, J., Petetin, H., McKeen, S., Beekmann, M., Warneke, C., Parrish, D. D., and de Gouw, J. A.: Emission ratios of anthropogenic volatile organic compounds in northern mid-latitude megacities: Observations versus emission inventories in Los Angeles and Paris, *J. Geophys. Res.*, 118, 2041–2057, <https://doi.org/10.1002/jgrd.50059>, 2013.
- Brock, F. V.: A Nonlinear Filter to Remove Impulse Noise from Meteorological Data, *J. Atmos. Ocean. Technol.*, 3, 51–58, [https://doi.org/10.1175/1520-0426\(1986\)003<0051:anftri>2.0.co;2](https://doi.org/10.1175/1520-0426(1986)003<0051:anftri>2.0.co;2), 1986.
- 20 Caplain, I., Cazier, F., Nouali, H., Mercier, A., Déchaux, J.-C., Nollet, V., Joumard, R., André, J.-M., and Vidon, R.: Emissions of unregulated pollutants from European gasoline and diesel passenger cars, *Atmos. Environ.*, 40, 5954–5966, <https://doi.org/10.1016/j.atmosenv.2005.12.049>, 2006.
- Chen, L. X., Dong, M., and Shao, Y. N.: The Characteristics Of Interannual Variations on the East Asian Monsoon, *J. Meteorol. Soc. Japan*, 25 70, 397–421, https://doi.org/10.2151/jmsj1965.70.1B_397, 1992.
- Cheng, J., Su, J., Cui, T., Li, X., Dong, X., Sun, F., Yang, Y., Tong, D., Zheng, Y., Li, Y., et al.: Dominant role of emission reduction in PM 2.5 air quality improvement in Beijing during 2013–2017: a model-based decomposition analysis, *Atmos. Chem. Phys.*, 19, 6125–6146, <https://doi.org/doi.org/10.5194/acp-19-6125-2019>, 2019.
- Deardorff, J. W.: Convective velocity and temperature scales for the unstable planetary boundary layer and for Rayleigh convection, *J. Atmos. Sci.*, 27, 1211–1213, [https://doi.org/10.1175/1520-0469\(1970\)027<1211:CVATSF>2.0.CO;2](https://doi.org/10.1175/1520-0469(1970)027<1211:CVATSF>2.0.CO;2), 1970.
- 30 Du, H., Li, J., Chen, X., Wang, Z., Sun, Y., Fu, P., Li, J., Gao, J., and Wei, Y.: Modeling of aerosol property evolution during winter haze episodes over a megacity cluster in northern China: roles of regional transport and heterogeneous reactions of SO₂, *Atmos. Chem. Phys.*, 19, 9351–9370, <https://doi.org/10.5194/acp-19-9351-2019>, 2019.
- Duan, J., Huang, R.-J., Li, Y., Chen, Q., Zheng, Y., Chen, Y., Lin, C., Ni, H., Wang, M., Ovadnevaite, J., et al.: Summertime and wintertime atmospheric processes of secondary aerosol in Beijing., *Atmos. Chem. Phys.*, 20, <https://doi.org/10.5194/acp-20-3793-2020>, 2020.
- European Database For Global Atmospheric Research: Global Emissions EDGAR v4.2, 2000–2012.

- Famulari, D., Nemitz, E., Di Marco, C., Phillips, G. J., Thomas, R., House, E., and Fowler, D.: Eddy-covariance measurements of nitrous oxide fluxes above a city, *Agric. For. Meteorol.*, 150, 786–793, <https://doi.org/10.1016/j.agrformet.2009.08.003>, 2010.
- Finnigan, J.: The storage term in eddy flux calculations, *Agric. For. Meteorol.*, 136, 108–113, <https://doi.org/10.1016/j.agrformet.2004.12.010>, 2006.
- 5 Foken, T.: *Micrometeorology*, Springer, Berlin, Heidelberg, Germany, 2 edn., <https://doi.org/10.1007/978-3-642-25440-6>, 2017.
- Foken, T. and Wichura, B.: Tools for quality assessment of surface-based flux measurements, *Agric. For. Meteorol.*, 78, 83–105, [https://doi.org/10.1016/0168-1923\(95\)02248-1](https://doi.org/10.1016/0168-1923(95)02248-1), 1996.
- Foken, T., Göckede, M., Mauder, M., Mahr, L., Amiro, B., and Munger, W.: Post-field data quality control in *Handbook of Micrometeorology*, in: *A Guide for Surface Flux Measurement and Analysis*, edited by Lee, X., Massman, W., and Law, B., pp. 181 – 208, Kluwer Academic Publisher, Dordrecht, <https://doi.org/10.1007/1-4020-2265-4>, 2004.
- 10 Gerbig, C., Kley, D., VolzThomas, A., Kent, J., Dewey, K., and McKenna, D. S.: Fast response resonance fluorescence CO measurements aboard the C-130: Instrument characterization and measurements made during North Atlantic Regional Experiment 1993, *J. Geophys. Res.*, 101, 29 229–29 238, <https://doi.org/10.1029/95jd03272>, 1996.
- Gerbig, C., Schmitgen, S., Kley, D., Volz-Thomas, A., Dewey, K., and Haaks, D.: An improved fast-response vacuum-UV resonance fluorescence CO instrument, *J. Geophys. Res.*, 104, 1699–1704, <https://doi.org/10.1029/1998jd100031>, 1999.
- 15 Guo, S., Hu, M., Zamora, M. L., Peng, J., Shang, D., Zheng, J., Du, Z., Wu, Z., Shao, M., Zeng, L., et al.: Elucidating severe urban haze formation in China, *pnas*, 111, 17 373–17 378, <https://doi.org/10.1073/pnas.1419604111>, 2014.
- Harrison, R. M., Dall’Osto, M., Beddows, D., Thorpe, A. J., Bloss, W. J., Allan, J. D., Coe, H., Dorsey, J. R., Gallagher, M., Martin, C., et al.: Atmospheric chemistry and physics in the atmosphere of a developed megacity (London): an overview of the REPARTEE experiment and its conclusions, *Atmos. Chem. Phys.*, 12, 3065–3114, <https://doi.org/10.5194/acp-12-3065-2012>, 2012.
- 20 Hartmann, J., Gehrmann, M., Kohnert, K., Metzger, S., and Sachs, T.: New calibration procedures for airborne turbulence measurements and accuracy of the methane fluxes during the AirMeth campaigns, *Atmos. Meas. Tech.*, 11, 4567–4581, <https://doi.org/10.5194/amt-11-4567-2018>, 2018.
- Heeb, N. V., Forss, A.-M., Bach, C., Reimann, S., Herzog, A., and Jäckle, H. W.: A comparison of benzene, toluene and C₂-benzenes mixing ratios in automotive exhaust and in the suburban atmosphere during the introduction of catalytic converter technology to the Swiss Car Fleet, *Atmos. Environ.*, 34, 3103–3116, [https://doi.org/10.1016/S1352-2310\(99\)00446-X](https://doi.org/10.1016/S1352-2310(99)00446-X), 2000.
- 25 Helfter, C., Tremper, A. H., Halios, C. H., Kotthaus, S., BJORKEGREN, A., GRIMMOND, C. S. B., BARLOW, J. F., and NEMITZ, E.: Spatial and temporal variability of urban fluxes of methane, carbon monoxide and carbon dioxide above London, UK, *Atmos. Chem. Phys.*, 16, 10 543–10 557, <https://doi.org/10.5194/acp-16-10543-2016>, 2016.
- 30 Jia, Y. T., Rahn, K. A., He, K. B., Wen, T. X., and Wang, Y. S.: A novel technique for quantifying the regional component of urban aerosol solely from its sawtooth cycles, *J. Geophys. Res.*, 113, <https://doi.org/10.1029/2008jd010389>, 2008.
- Jing, B. Y., Wu, L., Mao, H. J., Gong, S. N., He, J. J., Zou, C., Song, G. H., Li, X. Y., and Wu, Z.: Development of a vehicle emission inventory with high temporal-spatial resolution based on NRT traffic data and its impact on air pollution in Beijing - Part 1: Development and evaluation of vehicle emission inventory, *Atmos. Chem. Phys.*, 16, 3161–3170, <https://doi.org/10.5194/acp-16-3161-2016>, 2016.
- 35 Karl, T., Apel, E., Hodzic, A., Riemer, D., Blake, D., and Wiedinmyer, C.: Emissions of volatile organic compounds inferred from airborne flux measurements over a megacity, *Atmos. Chem. Phys.*, 9, 271–285, <https://doi.org/10.5194/acp-9-271-2009>, 2009.

- Karl, T., Graus, M., Striednig, M., Lamprecht, C., Hammerle, A., Wohlfahrt, G., Held, A., von der Heyden, L., Deventer, M. J., Krismer, A., Haun, C., Feichter, R., and Lee, J.: Urban eddy covariance measurements reveal significant missing NO_x emissions in Central Europe, *Sci. Rep.*, 7, <https://doi.org/10.1038/s41598-017-02699-9>, 2017.
- Karl, T., Striednig, M., Graus, M., Hammerle, A., and Wohlfahrt, G.: Urban flux measurements reveal a large pool of oxygenated volatile organic compound emissions, *Proc. Nat. Acad. Sci. USA*, 115, 1186–1191, <https://doi.org/10.1073/pnas.1714715115>, 2018.
- Kljun, N., Calanca, P., Rotach, M. W., and Schmid, H. P.: A simple parameterisation for flux footprint predictions, *Bound.-Lay. Meteorol.*, 112, 503–523, <https://doi.org/10.1023/b:boun.0000030653.71031.96>, 2004.
- Kotthaus, S. and Grimmond, C. S. B.: Atmospheric boundary-layer characteristics from ceilometer measurements. Part 1: A new method to track mixed layer height and classify clouds, *Quarterly Journal of the Royal Meteorological Society*, 144, 1525–1538, <https://doi.org/10.1002/qj.3299>, 2018.
- Krotkov, N. A., McLinden, C. A., Li, C., Lamsal, L. N., Celarier, E. A., Marchenko, S. V., Swartz, W. H., Bucsela, E. J., Joiner, J., Duncan, B. N., Boersma, K. F., Veefkind, J. P., Levelt, P. F., Fioletov, V. E., Dickerson, R. R., He, H., Lu, Z. F., and Streets, D. G.: Aura OMI observations of regional SO₂ and NO₂ pollution changes from 2005 to 2015, *Atmos. Chem. Phys.*, 16, 4605–4629, <https://doi.org/10.5194/acp-16-4605-2016>, 2016.
- Langford, B., Davison, B., Nemitz, E., and Hewitt, C. N.: Mixing ratios and eddy covariance flux measurements of volatile organic compounds from an urban canopy (Manchester, UK), *Atmos. Chem. Phys.*, 9, 1971–1987, <https://doi.org/10.5194/acp-9-1971-2009>, 2009.
- Langford, B., Nemitz, E., House, E., Phillips, G. J., Famulari, D., Davison, B., Hopkins, J. R., Lewis, A. C., and Hewitt, C. N.: Fluxes and concentrations of volatile organic compounds above central London, UK, *Atmos. Chem. Phys.*, 10, 627–645, <https://doi.org/10.5194/acp-10-627-2010>, 2010.
- Langford, B., Acton, J., Ammann, C., Valach, A., and Nemitz, E.: Eddy-covariance data with low signal-to-noise ratio: time-lag determination, uncertainties and limit of detection, *Atmos. Meas. Tech.*, 8, 4197–4213, <https://doi.org/10.5194/amt-8-4197-2015>, 2015.
- Lee, J. D., Moller, S. J., Read, K. A., Lewis, A. C., Mendes, L., and Carpenter, L. J.: Year-round measurements of nitrogen oxides and ozone in the tropical North Atlantic marine boundary layer, *J. Geophys. Res.*, 114, <https://doi.org/10.1029/2009jd011878>, 2009.
- Lee, J. D., Helfter, C., Purvis, R. M., Beevers, S. D., Carslaw, D. C., Lewis, A. C., Moller, S. J., Tremper, A., Vaughan, A., and Nemitz, E. G.: Measurement of NO_x Fluxes from a Tall Tower in Central London, UK and Comparison with Emissions Inventories, *Environ. Sci. Technol.*, 49, 1025–1034, <https://doi.org/10.1021/es5049072>, 2015.
- Lee, X., Massman, W., and Law, B.: *Handbook of Micrometeorology: A Guide for Surface Flux Measurement and Analysis*, Atmospheric and Oceanographic Sciences Library, Springer Netherlands, Dordrecht, The Netherlands, <https://doi.org/10.1007/1-4020-2265-4>, 2004.
- Li, H. Y., Zhang, Q., Chen, C. R., Wang, L. T., Wei, Z., Zhou, S., Parworth, C., Zheng, B., Canonaco, F., Prevot, A. S. H., Chen, P., Zhang, H. L., Wallington, T. J., and He, K. B.: Wintertime aerosol chemistry and haze evolution in an extremely polluted city of the North China Plain: significant contribution from coal and biomass combustion, *Atmos. Chem. Phys.*, 17, 4751–4768, <https://doi.org/10.5194/acp-17-4751-2017>, 2017.
- Liu, C., Yin, P., Chen, R., Meng, X., Wang, L., Niu, Y., Lin, Z., Liu, Y., Liu, J., and Qi, J.: Ambient carbon monoxide and cardiovascular mortality: a nationwide time-series analysis in 272 cities in China, *Lancet Planet. Health*, 2, e12–e18, [https://doi.org/10.1016/S2542-5196\(17\)30181-X](https://doi.org/10.1016/S2542-5196(17)30181-X), 2018.
- Liu, F., Zhang, Q., Ronald, J. V., Zheng, B., Tong, D., Yan, L., Zheng, Y. X., and He, K. B.: Recent reduction in NO_x emissions over China: synthesis of satellite observations and emission inventories, *Environ. Res. Lett.*, 11, 114002, <https://doi.org/10.1088/1748-9326/11/11/114002>, 2016.

- Liu, H. Z., Feng, J. W., Jarvi, L., and Vesala, T.: Four-year (2006–2009) eddy covariance measurements of CO₂ flux over an urban area in Beijing, *Atmos. Chem. Phys.*, 12, 7881–7892, <https://doi.org/10.5194/acp-12-7881-2012>, 2012.
- Mann, J. and Lenschow, D. H.: Errors in airborne flux measurements, *J. Geophys. Res.*, 99, 14 519–14 526, <https://doi.org/10.1029/94jd00737>, 1994.
- 5 Marr, L. C., Moore, T. O., Klappmeyer, M. E., and Killar, M. B.: Comparison of NO_x Fluxes Measured by Eddy Covariance to Emission Inventories and Land Use, *Environ. Sci. Technol.*, 47, 1800–1808, <https://doi.org/10.1021/es303150y>, 2013.
- McDonald, B. C., de Gouw, J. A., Gilman, J. B., Jathar, S. H., Akherati, A., Cappa, C. D., Jimenez, J. L., Lee-Taylor, J., Hayes, P. L., McKeen, S. A., et al.: Volatile chemical products emerging as largest petrochemical source of urban organic emissions, *Science*, 359, 760–764, <https://doi.org/10.1126/science.aag0524>, 2018.
- 10 Metzger, S., Junkermann, W., Mauder, M., Beyrich, F., Butterbach-Bahl, K., Schmid, H. P., and Foken, T.: Eddy-covariance flux measurements with a weight-shift microlight aircraft, *Atmos. Meas. Tech.*, 5, 1699–1717, <https://doi.org/10.5194/amt-5-1699-2012>, 2012.
- Metzger, S., Durden, D., Sturtevant, C., Luo, H., Pingingtha-Durden, N., Sachs, T., Serafimovich, A., Hartmann, J., Li, J. H., Xu, K., and Desai, A. R.: eddy4R 0.2.0: a DevOps model for community-extensible processing and analysis of eddy-covariance data based on R, Git, Docker, and HDF5, *Geosci. Model Dev.*, 10, 3189–3206, <https://doi.org/10.5194/gmd-10-3189-2017>, 2017.
- 15 Ministry of Ecology and Environment, the People’s Republic of China: 2017 Report on the State of the Ecology and Environment in China, 2018.
- Miyazaki, K., Eskes, H., Sudo, K., Boersma, K. F., Bowman, K., and Kanaya, Y.: Decadal changes in global surface NO_x emissions from multi-constituent satellite data assimilation, *Atmos. Chem. Phys.*, 17, 807–837, <https://doi.org/10.5194/acp-17-807-2017>, 2017.
- Moravek, A., Singh, S., Pattey, E., Pelletier, L., and Murphy, J. G.: Measurements and quality control of ammonia eddy covariance fluxes: a new strategy for high-frequency attenuation correction, *Atmos. Meas. Tech.*, 12, 6059–6078, <https://doi.org/10.5194/amt-12-6059-2019>, 2019.
- 20 Nordbo, A. and Katul, G.: A wavelet-based correction method for eddy-covariance high-frequency losses in scalar concentration measurements, *Bound.-Lay. Meteorol.*, 146, 81–102, <https://doi.org/10.1007/s10546-012-9759-9>, 2013.
- Park, C., Schade, G. W., and Boedeker, I.: Flux measurements of volatile organic compounds by the relaxed eddy accumulation method combined with a GC-FID system in urban Houston, Texas, *Atmos. Environ.*, 44, 2605–2614, <https://doi.org/10.1016/j.atmosenv.2010.04.016>, 2010.
- 25 Parrish, D. D., Kuster, W. C., Shao, M., Yokouchi, Y., Kondo, Y., Goldan, P. D., de Gouw, J. A., Koike, M., and Shirai, T.: Comparison of air pollutant emissions among mega-cities, *Atmos. Environ.*, 43, 6435–6441, <https://doi.org/10.1016/j.atmosenv.2009.06.024>, 2009.
- Pattey, E., Desjardins, R. L., Boudreau, F., and Rochette, P.: Impact of density fluctuations on flux measurements of trace gases: Implications for the relaxed eddy accumulation technique, *Bound.-Lay. Meteorol.*, 59, 195–203, <https://doi.org/10.1007/BF00120695>, 1992.
- 30 Qi, J., Zheng, B., Li, M., Yu, F., Chen, C., Liu, F., Zhou, X., Yuan, J., Zhang, Q., and He, K.: A high-resolution air pollutants emission inventory in 2013 for the Beijing-Tianjin-Hebei region, China, *Atmos. Environ.*, 170, 156–168, <https://doi.org/10.1016/j.atmosenv.2017.09.039>, 2017.
- Rantala, P., Järvi, L., Taipale, R., Laurila, T. K., Patokoski, J., Kajos, M. K., Kurppa, M., Haapanala, S., Siivola, E., Petäjä, T., et al.: Anthropogenic and biogenic influence on VOC fluxes at an urban background site in Helsinki, Finland, *Atmos. Chem. Phys.*, 16, 7981–8007, <https://doi.org/10.5194/acp-16-7981-2016>, 2016.

- Saikawa, E., Kim, H., Zhong, M., Avramov, A., Zhao, Y., Janssens-Maenhout, G., Kurokawa, J.-i., Klimont, Z., Wagner, F., and Naik, V.: Comparison of emissions inventories of anthropogenic air pollutants and greenhouse gases in China, *Atmos. Chem. Phys.*, 17, 6393, <https://doi.org/10.5194/acp-17-6393-2017>, 2017.
- Shi, Z., Vu, T., Kotthaus, S., Harrison, R. M., Grimmond, S., Yue, S., Zhu, T., Lee, J., Han, Y., Demuzere, M., et al.: Introduction to the special issue “In-depth study of air pollution sources and processes within Beijing and its surrounding region (APHH-Beijing)”, *Atmos. Chem. Phys.*, 19, 7519–7546, <https://doi.org/10.5194/acp-19-7519-2019>, 2019.
- Starkenburg, D., Metzger, S., Fochesatto, G. J., Alfieri, J. G., Gens, R., Prakash, A., and Cristobal, J.: Assessment of Despiking Methods for Turbulence Data in Micrometeorology, *J. Atmos. Ocean. Technol.*, 33, 2001–2013, <https://doi.org/10.1175/jtech-d-15-0154.1>, 2016.
- Strand, V., Svartengren, M., Rak, S., Barck, C., and Bylin, G.: Repeated exposure to an ambient level of NO₂ enhances asthmatic response to a nonsymptomatic allergen dose, *Eur. Respir. J.*, 12, 6–12, <https://doi.org/10.1183/09031936.98.12010006>, 1998.
- Tunncliffe, W. S., Burge, P. S., and Ayres, J. G.: Effect of domestic concentrations of nitrogen dioxide on airway responses to inhaled allergen in asthmatic patients, *Lancet*, 344, 1733–1736, [https://doi.org/10.1016/s0140-6736\(94\)92886-x](https://doi.org/10.1016/s0140-6736(94)92886-x), 1994.
- United Nations’ Department Of Economic and Social Affairs: Population Division: The World’s Cities in 2016, 2016.
- Valach, A., Langford, B., Nemitz, E., MacKenzie, A. R., and Hewitt, C. N. P.: Seasonal and diurnal trends in concentrations and fluxes of volatile organic compounds in central London, *Atmos. Chem. Phys.*, 15, 7777–7796, <https://doi.org/10.5194/acp-15-7777-2015>, 2015.
- Vaughan, A. R., Lee, J. D., Misztal, P. K., Metzger, S., Shaw, M. D., Lewis, A. C., Purvis, R. M., Carslaw, D. C., Goldstein, A. H., Hewitt, C. N., Davison, B., Beevers, S. D., and Karl, T. G.: Spatially resolved flux measurements of NO_x from London suggest significantly higher emissions than predicted by inventories, *Faraday Discuss.*, 189, 455–472, <https://doi.org/10.1039/c5fd00170f>, 2016.
- Vaughan, A. R., Lee, J. D., Shaw, M. D., Misztal, P. K., Metzger, S., Vieno, M., Davison, B., Karl, T. G., Carpenter, L. J., Lewis, A. C., Purvis, R. M., Goldstein, A. H., and Hewitt, C. N.: VOC emission rates over London and South East England obtained by airborne eddy covariance, *Faraday Discuss.*, 200, 599–620, <https://doi.org/10.1039/c7fd00002b>, 2017.
- Velasco, E., Lamb, B., Pressley, S., Allwine, E., Westberg, H., Jobson, B., Alexander, M., Prazeller, P., Molina, L., and Molina, M.: Flux measurements of volatile organic compounds from an urban landscape, *Geophys. Res. Lett.*, 32, L20 802, <https://doi.org/10.1029/2005GL023356>, 2005.
- Velasco, E., Pressley, S., Grivicke, R., Allwine, E., Coons, T., Foster, W., Jobson, B., Westberg, H., Ramos, R., Hernández, F., et al.: Eddy covariance flux measurements of pollutant gases in urban Mexico City, *Atmos. Chem. Phys.*, 9, 7325–7342, <https://doi.org/10.5194/acp-9-7325-2009>, 2009.
- von Schneidmesser, E., Monks, P. S., and Plass-Duelmer, C.: Global comparison of VOC and CO observations in urban areas, *Atmos. Environ.*, 44, 5053–5064, <https://doi.org/10.1016/j.atmosenv.2010.09.010>, 2010.
- Wang, P., Elansky, N., Timofeev, Y. M., Wang, G., Golitsyn, G., Makarova, M., Rakitin, V., Shtabkin, Y., Skorokhod, A., Grechko, E., et al.: Long-Term Trends of Carbon Monoxide Total Columnar Amount in Urban Areas and Background Regions: Ground-and Satellite-based Spectroscopic Measurements, *Adv. Atmos. Sci.*, 35, 785–795, <https://doi.org/10.1007/s00376-017-6327-8>, 2018.
- Wang, S. X., Zhao, M., Xing, J., Wu, Y., Zhou, Y., Lei, Y., He, K. B., Fu, L. X., and Hao, J. M.: Quantifying the Air Pollutants Emission Reduction during the 2008 Olympic Games in Beijing, *Environ. Sci. Technol.*, 44, 2490–2496, <https://doi.org/10.1021/es9028167>, 2010.
- Webb, E. K., Pearman, G. I., and Leuning, R.: Correction of flux measurements for density effects due to heat and water vapour transfer, *Quart. J. Roy. Meteorol. Soc.*, 106, 85–100, <https://doi.org/10.1002/qj.49710644707>, 1980.

- Yang, Z., Wang, H., Shao, Z., and Muncrief, R.: Review of Beijing's Comprehensive Motor Vehicle Emission Control Programs, Tech. rep., International Council on Clean Transportation, <https://theicct.org/publications/review-beijings-comprehensive-motor-vehicle-emission-control-programs>, 2015.
- 5 Zhao, Y., Zhou, Y. D., Qiu, L. P., and Zhang, J.: Quantifying the uncertainties of China's emission inventory for industrial sources: From national to provincial and city scales, *Atmos. Environ.*, 165, 207–221, <https://doi.org/10.1016/j.atmosenv.2017.06.045>, 2017.
- Zheng, B., Zhang, Q., Tong, D., Chen, C., Hong, C., Li, M., Geng, G., Lei, Y., Huo, H., and He, K.: Resolution dependence of uncertainties in gridded emission inventories: a case study in Hebei, China, *Atmos. Chem. Phys.*, 17, 921–933, <https://doi.org/10.5194/acp-17-921-2017>, 2017.
- 10 Zheng, B., Chevallier, F., Ciais, P., Yin, Y., Deeter, M. N., Worden, H. M., Wang, Y., Zhang, Q., and He, K.: Rapid decline in carbon monoxide emissions and export from East Asia between years 2005 and 2016, *Environ. Res. Lett.*, 13, 044 007, <https://doi.org/10.1088/1748-9326/aab2b3>, 2018.